

(3*R*,5*S*,*E*)-7-(4-(4-Fluorophenyl)-6-isopropyl-2-(methyl(1-methyl-1*H*-1,2,4-triazol-5-yl)amino)pyrimidin-5-yl)-3,5-dihydroxyhept-6-enoic Acid (BMS-644950): A Rationally Designed Orally Efficacious 3-Hydroxy-3-methylglutaryl Coenzyme-A Reductase Inhibitor with Reduced Myotoxicity Potential

Saleem Ahmad,* Cort S. Madsen,[†] Philip D. Stein, Evan Janovitz, Christine Huang, Khehyong Ngu, Sharon Bisaha, Lawrence J. Kennedy, Bang-Chi Chen, Rulin Zhao, Doree Sitkoff, Hossain Monshizadegan, Xiaohong Yin, Carol S. Ryan, Rongan Zhang, Mary Giancarli, Eileen Bird, Ming Chang, Xing Chen, Robert Setters, Debra Search, Shaobin Zhuang, Van Nguyen-Tran, Carolyn A. Cuff, Thomas Harrity, Celia J. Darienzo, Tong Li, Richard A. Reeves, Michael A. Blanar, Joel C. Barrish, Robert Zahler, and Jeffrey A. Robl

Bristol-Myers Squibb Research & Development, P.O. Box 4000, Princeton, New Jersey 08543

Received January 2, 2008

3-Hydroxy-3-methylglutaryl coenzyme-A reductase (HMGR) inhibitors, more commonly known as statins, represent the gold standard in treating hypercholesterolemia. Although statins are regarded as generally safe, they are known to cause myopathy and, in rare cases, rhabdomyolysis. Statin-dependent effects on plasma lipids are mediated through the inhibition of HMGR in the hepatocyte, whereas evidence suggests that myotoxicity is due to inhibition of HMGR within the myocyte. Thus, an inhibitor with increased selectivity for hepatocytes could potentially result in an improved therapeutic window. Implementation of a strategy that focused on *in vitro* potency, compound polarity, cell selectivity, and oral absorption, followed by extensive efficacy and safety modeling in guinea pig and rat, resulted in the identification of compound **1b** (BMS-644950). Using this discovery pathway, we compared **1b** to other marketed statins to demonstrate its outstanding efficacy and safety profile. With the potential to generate an excellent therapeutic window, **1b** was advanced into clinical development.

Introduction

The risk for coronary heart disease is increased in individuals with elevated concentrations of plasma low-density lipoprotein-cholesterol (LDL-C^a).¹ Inhibition of HMGR, the rate-limiting enzyme in cholesterol biosynthesis, has proven to be one of the most effective approaches for lowering plasma LDL-C and reducing cardiovascular event rates.² As part of a compensatory mechanism to sterol depletion in the liver, inhibition of HMGR ultimately leads to the increased production of LDL receptors and subsequent clearance of LDL-C from systemic circulation.³ Although this compensatory mechanism is highly complex and not fully understood, it has been suggested that sterol depletion caused by HMGR inhibition activates the sterol response element binding protein (SREBP), a transcription factor that promotes expression of the LDL-receptor gene.⁴

HMGR inhibitors (statins) represent the gold standard in treating hypercholesterolemia and mixed dyslipidemia. The first-generation statins such as simvastatin,⁵ pravastatin,⁶ lovastatin,⁷ and fluvastatin⁸ show a modest ability to lower lipids in man (LDL-C reduction 20–40%).⁹ Often referred to as “superstatins”, the second-generation statins, such as atorvastatin,¹⁰ cerivastatin (marketing discontinued),¹¹ and rosuvastatin,¹² elicit greater reductions in LDL-C (40–60%).¹³ Several landmark clinical trials have firmly established the effectiveness of statins in lowering LDL-C and reducing overall mortality and cardiovas-

cular events.¹⁴ Current guidelines from the National Cholesterol Education Program emphasize the need for aggressive lipid lowering in patients with multiple risk factors, such as previous heart attack, hypertension, or diabetes mellitus. For these high-risk patients, the optimal goal for LDL-C is <100 mg/dL, as compared to the previous goal of <130 mg/dL. Under these guidelines it is expected that achieving good treatment-to-goal success rates will require statins with greater LDL-C-reducing capacity, similar to atorvastatin and rosuvastatin.¹⁵ Thus, the rationale for statin-based therapies, and perhaps even more so superstatin-based therapies, has only increased with accumulating clinical data.

Although statins are regarded as generally safe, skeletal muscle-related toxicity remains an associated adverse effect. Important for the clinical diagnosis of skeletal muscle toxicity is the biochemical marker creatine kinase (CK). Creatine kinase generates adenosine triphosphate via phosphorylation of adenosine diphosphate and is primarily found in skeletal muscle and the myocardium. Plasma levels of CK rise after muscle cell membrane damage and subsequent leakage into the systemic circulation. A review of the data from multiple clinical trials involving statin therapy found that myalgia (muscle pain) may affect an estimated 1% to 5% of patients.¹⁶ Although the definition varies among studies, myopathy has traditionally been defined as CK levels greater than 10 times the upper limit of normal accompanied by symptoms (e.g., generalized myalgia, fatigue, or muscle weakness).¹⁷ Myopathy is estimated to occur in approximately 0.1% of patients who receive statin monotherapy.¹⁸ If myopathy is not recognized and therapy is continued, it can progress further to life-threatening rhabdomyolysis.¹⁹

Rhabdomyolysis is a clinical syndrome that results from severe and widespread necrosis of skeletal muscle with subse-

* To whom correspondence should be addressed. Phone: 609-252-6955. Fax: 609-252-6804. E-mail: saleem.ahmad@bms.com.

[†] Equal contributing author.

^a Abbreviations used: LDL-C, low-density lipoprotein-cholesterol; HMGR, 3-hydroxy-3-methylglutaryl coenzyme-A reductase; CK, creatine kinase; OATP, organic anion transporter polypeptide; TEMPO, 2,2,6,6-tetramethylpiperidine 1-oxyl; TC, total cholesterol; ALT, alanine aminotransferase; AST, aspartate aminotransferase; P-gp, P-glycoprotein.

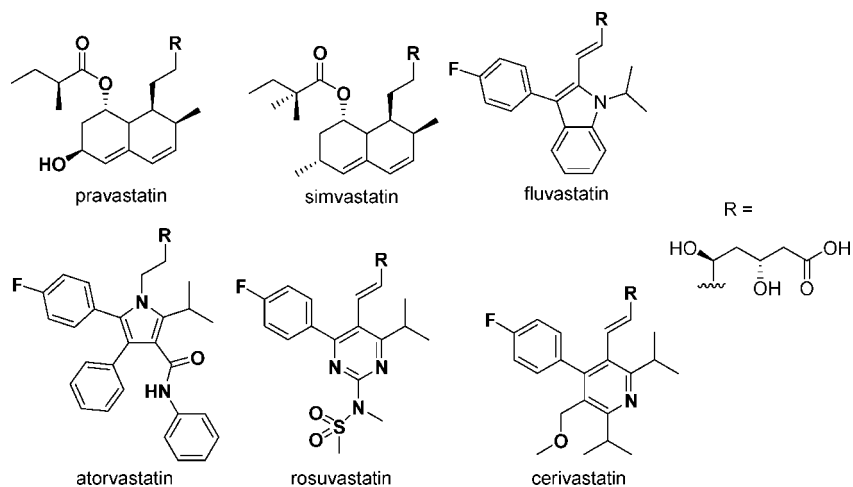


Figure 1. Structures of five major marketed statins and cerivastatin (which was withdrawn from the market in 2001). Simvastatin is administered as the corresponding lactone form of the dihydroxy acid.

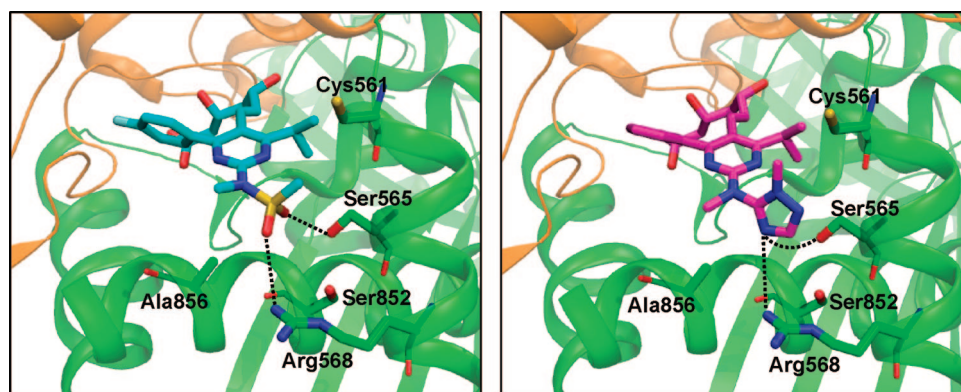


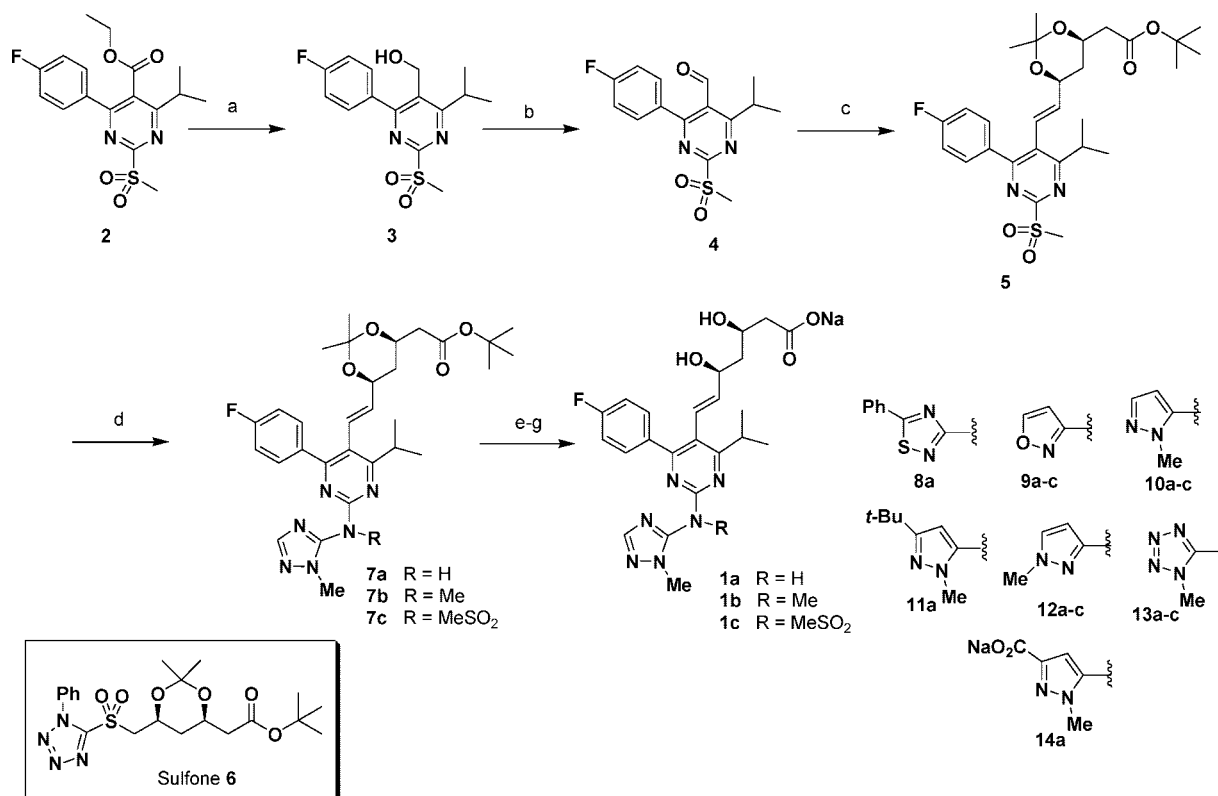
Figure 2. (Left) X-ray crystal structure of rosuvastatin (cyan) bound between two monomers of HMGR (green and orange).²⁶ The dotted black lines represent a putative hydrogen bond between one oxygen of the ligand's methanesulfonyl group and the Ser565 side chain (2.7 Å), and a favorable electrostatic interaction between the other oxygen of the methanesulfonyl group and Arg568 (3.8 Å to closest atom). Additional side chains having favorable contacts with the ligand's *N*-(methyl)methanesulfonyl group are shown in stick representation; Ser852 does not contact the ligand but is depicted for clarity. (Right) Compound 1b (magenta) is shown modeled into the HMGR active site.²⁷ Favorable electrostatic interactions between the denoted nitrogen and Ser565 side chain (3.6 Å) as well as to Arg568 (4.2 Å to closest atom) are represented by dotted black lines. Additional side chains having favorable contacts with the *N*-(methyl)triazole ring are shown in stick representation.

quent release of intracellular elements leading to acute renal failure. Cases of statin-induced rhabdomyolysis are rare; yet, because fatalities have occurred, rhabdomyolysis represents an important concern for physicians prescribing this class of drugs. Despite extensive research, the exact mechanism(s) of statin-induced myotoxicity remains elusive.^{20,21} However, data suggest that the toxicological effects of statins on the myocyte are the direct result of HMGR inhibition and subsequent reduction of downstream metabolites, and are not due to the lowering of plasma cholesterol levels.²² Although statins have been utilized successfully for nearly two decades, the withdrawal of cerivastatin, due to its unacceptable myotoxicity profile, has led to a greater appreciation that all statins are not equal with regard to potential for serious adverse events. The ability to differentiate statins at the preclinical stage is critical to successfully identifying new and safer drug candidates within this class.

As part of the scientific rationale for the development of a superstatin with an improved muscle safety profile, the focus of our program involved implementing a compound design strategy based on (1) minimizing peripheral exposure and (2) reducing the capacity for muscle cell penetrance by altering compound lipophilicity. While hydrophilic statins (e.g., pravastatin and rosuvastatin) probably enter the hepatocytes (but not

myocytes) via an active transport mechanism involving organic anion transporter polypeptide (OATP), hydrophobic statins (e.g., cerivastatin) enter hepatocytes via passive diffusion.^{23,24} A main focus of our program was based on the hypothesis that, unlike lipophilic compounds, more polar molecules would have diminished cell permeability in myocytes resulting in improved cell selectivity.²⁵ To aid in this effort, a thorough examination of the X-ray crystal structures of various enzyme-bound statins was carried out in order to identify polar regions within the ligand binding site of HMGR that could tolerate or favor polar groups on a ligand. Of particular interest was the crystal structure of rosuvastatin, where a pendant methanesulfonyl group occupies a binding site adjacent to the side chains of serine565 and arginine568 (Figure 2). Molecular modeling revealed that a small (five- or six-membered ring) heterocycle with optimally placed heteroatoms would likely capitalize on potential binding interactions similar to those observed with rosuvastatin. The nature of the heterocycle along with its substituents could then be used to modulate hydrophilicity and selectivity of the molecules.

In order to expeditiously test the hypothesis, we designed an approach that would introduce a variety of heterocycles at a late stage of the synthesis, thereby avoiding a lengthy multistep

Scheme 1^a

^a Reagents: (a) DIBAL/methylene chloride, 61%; (b) TEMPO/buffered bleach/EtOAc, 100% (unpurified); (c) sulfone **6**/LiHMDS/THF, 99%; (d) 1-methyl-1*H*-1,2,4-triazol-5-amine/LiN(TMS)₂/THF or DMF; (e) LiN(TMS)₂/MeI or MeSO₂Cl/THF or DMF; (f) HCl/THF; (g) NaOH/THF–MeOH (35–70% from **5**).

route to these highly complex molecules. This effort, coupled with extensive *in vitro* and *in vivo* safety characterization, resulted in the identification of compound **1b** (BMS-644950) as a novel, potent, and efficacious HMGR inhibitor with a potentially superior safety profile.

Chemistry

A wide variety of novel chemotypes were developed during the course of this program to explore the effect of structural modification and polarity on *in vitro* potency, selectivity, and *in vivo* efficacy. The approach depicted in Scheme 1 involved the utilization of the advanced intermediate **5**, which was readily converted to the various heterocyclic analogues to facilitate rapid SAR development. Intermediate **5** was prepared in three steps from the previously reported pyrimidine **2**.²⁸ Diisobutylaluminum hydride reduction of **2** afforded alcohol **3**, which was oxidized to the corresponding aldehyde **4** using TEMPO (2,2,6,6-tetramethylpiperidine 1-oxyl) and buffered bleach. Aldehyde **4** was converted to intermediate **5** via Julia/Kocienski^{29,30} olefination using the previously described sulfone **6**.³¹ Treatment of **5** with the anion of 1-methyl-1*H*-1,2,4-triazol-5-amine (generated via deprotonation with LiN(TMS)₂) afforded **7a** in 73% yield. The reaction could be carried out by treating 1-methyl-1*H*-1,2,4-triazol-5-amine with LiN(TMS)₂ in THF or DMF prior to the addition of the sulfone **5**, or alternatively by addition of LiN(TMS)₂ to a solution of **5** and 1-methyl-1*H*-1,2,4-triazol-5-amine. Intermediate **7a** could be converted directly to the final compound **1a** by deprotection of the side chain via sequential treatment with HCl and NaOH. Alternatively **7a** could be converted to **7b** (R = Me) or **7c** (R = MeSO₂) by treatment with LiN(TMS)₂ and methyl iodide or methanesulfonyl chloride prior to deprotection of the side chain to access

compounds **1b** and **1c**. In a similar fashion, other amino heterocycles could be utilized in this sequence to generate compounds **8–14**.

Results and Discussion

In Vitro Studies/SARs. The primary screens utilized have been described in detail elsewhere and references therein.³² Rat HMGR enzyme derived from liver microsomes was utilized to directly measure enzyme inhibition. Freshly isolated hepatocytes from rat and rat L6 myocytes grown in culture were utilized to measure inhibition of cholesterol synthesis within the cell (Table 1). The ratio of the L6 myocyte IC₅₀ to rat hepatocyte IC₅₀ (cell selectivity) was used as an indicator of myotoxic potential. A variety of marketed statins were assayed in these *in vitro* screens to enable a comparative evaluation versus our program compounds. As anticipated, the more lipophilic statins (e.g., cerivastatin) exhibited the lowest cell selectivity, whereas the more polar statins (e.g., pravastatin and rosuvastatin) were identified as being highly selective in these cell-based models. To measure polarity, a high-throughput reversed-phase HPLC-based log *P* assay³³ was used for routine screening. The assay was validated by comparing the data obtained for known statins with the data from traditional octanol–water partitioning.³⁴ Figure 3 displays a plot of the two sets of log *P* values showing a good correlation ($R^2 = 0.98$).

Most of the novel compounds met our *in vitro* potency criteria, showing good enzyme-inhibitory and comparable hepatocyte activities (Table 1). The *in vitro* activity did not vary significantly by modifying the heterocyclic rings. This finding could be related to the permissive nature of the larger binding site where this group resides. In contrast, the nature of the heterocycles along with their substituents extensively modulated

Table 1. In Vitro Rat Enzyme, Rat Hepatocyte, Rat L6-Myocyte, and in Vivo Rat Data: Effect of Partitioning Coefficient (log *P*) on Cell Selectivity

compd	enzyme IC ₅₀ ^a (nM)	hepatocytes IC ₅₀ ^b (nM)	myocytes IC ₅₀ ^b (nM)	cell selectivity ratio	HPLClog <i>P</i> ^c	rat ED ₅₀ or % inhib at 1 mg/kg ^d
8a ^e	6.9 ± 0.3	7.7	7.1 ± 1.9	0.9	4.0	20%
9a	2.3 ± 0.5	1.4 ± 0.5	132 ± 14	94	2.4	43%
9b	7.0 ± 1.8	9	41	4.6	3.5	ND
9c	33.0 ± 13	5.5 ± 1.7	> 1000	> 181.8	1.8	64%
10a	2.4 ± 0.9	1.3 ± 0.2	55 ± 4	42	2.2	60%
10b	2.5 ± 0.1	2.5 ± 1.3	135 ± 29	54	3.14	86%
10c	2.2	5.4 ± 1.9	6277 ± 3176	1162	1.79	61%
11a	12.4 ± 0.7	1.9	4.9	2.6	3.7	54%
12a	1.8 ± 0.1	3.7 ± 1.9	1034 ± 342	279	2.3	62%
12b	2.5 ± 0.0	1.2 ± 0.2	63 ± 3	53	3.18	67%
12c	3.7 ± 0.1	7.7	> 10 000	> 1299	1.33	23%
13a	0.9 ± 0.4	1.5 ± 0.5	2289	1526	1.3	50%
13b	0.5	1.4 ± 0.1	983 ± 55	702	2.0	0.067 mg/kg
13c	4.2	1.0 ± 0.3	3138 ± 832	3138	1.84	42%
14a	0.9 ± 0.0	13.7 ± 1.2	> 10 000	> 730	-0.1	55%
1a	3.0	3.7 ± 0.2	2778 ± 61	751	1.12	ND
1c	2.9 ± 0.1	7.5 ± 1.9	> 10 000	> 1333	1.7	24%
1b	1.4 ± 0.4	3.95 ± 0.8	995 ± 53	252	2.16 (0.3)	0.11 mg/kg
atorvastatin	6.2 ± 1.7	2.5 ± 0.8	78 ± 22	31	3.76 (1.2)	0.26 mg/kg
rosuvastatin	3.1 ± 0.4	0.6 ± 0.1	65 ± 17	108	2.4 (-0.37)	0.35 mg/kg
simvastatin	4.3 ± 1.3	6.2 ± 1.3	27 ± 0.8	4.4	4.84 (1.81)	0.40 mg/kg
cerivastatin	9.8 ± 2.8	2.3 ± 0.4	1.7 ± 0.9	0.7	4.49 (1.66)	0.09 mg/kg
pravastatin	31.6 ± 4.4	29 ± 4	1519 ± 514	52	2.2 (-0.67)	0.68 mg/kg

^a HMGR activity was measured using a previously described method.³⁵ Rat hepatic microsomes were used as the source of the enzyme, and activity was determined by measuring the conversion of ¹⁴C-HMG-CoA to ¹⁴C-mevalonic acid. IC₅₀ values were generated from 10-point dose–response curves (*n* ≥ 2). ^b Cellular synthesis of cholesterol was measured as incorporation of ¹⁴C-acetate into cholesterol in rat hepatocytes and rat L6 myocytes (a rat skeletal muscle cell line) using an adaptation from a previously described method.³⁶ Effects are expressed as mean IC₅₀ values (concentration of drug producing 50% inhibition of cholesterol synthesis) based on 6-point dose–response curves derived from independent experiments (*n* ≥ 2). ^c Log *P* was measured for hydroxy acid forms by the HPLC method;³³ values in parentheses are derived from octanol–buffer measurements reported in the literature³⁴ (except for compound **1b**, which was determined in-house). ^d In vivo inhibition of hepatic cholesterol synthesis in rats as determined from a 4- to 6-point dose–response curve (*n* = 5 animals/dose group). ND = not determined. ^e Series a (R = H), b (R = Me), c (R = SO₂Me).

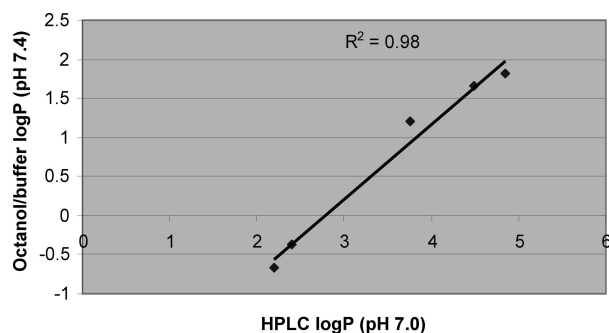


Figure 3. Correlation of log *P* values as measured by octanol–water partitioning and HPLC methods (log *P* values: octanol–water (pH 7.4 buffer)/HPLC (pH 7.0); pravastatin -0.67/2.2, rosuvastatin -0.37/2.4, atorvastatin 1.2/3.76, simvastatin sodium 1.81/4.84, cerivastatin 1.66/4.49).

the polarity of compounds, providing a diverse set of analogues with a broad range of log *P* values. In general, high cellular selectivity ratios correlated well with decreasing log *P* values. This correlation was observed for both the reference statins and program compounds. The noted difference in activities between cell types as related to compound polarity has been attributed to the presence of endogenous transporters (e.g., OATPs)^{23,24} in hepatocytes, which allow for active transport of these compounds into the cell. In contrast, the myocyte is thought to be devoid of the related transporter mechanisms. Increasing

polarity thus attenuates permeability in myocytes but not in hepatocytes, leading to the observed selectivity ratios. Overall, compounds with HPLC log *P* values > 3.0 (e.g., compound **10b**, selectivity = 54, HPLC log *P* = 3.14) did not meet our in vitro cell selectivity target of > 100. Nonetheless, evaluation in these in vitro screens provided numerous compounds, including **1b**, with excellent enzymatic potency and a desirable cell selectivity profile, which were suitable for evaluation in subsequent in vivo efficacy and safety studies.

In Vivo Efficacy in the Acute Rat Model. Multiple compounds met our criteria for in vitro potency and cell selectivity. Thus, a medium-throughput in vivo rat assay (as described in Experimental Section) was used to further differentiate program compounds. Acute inhibition of cholesterol synthesis, as indicated by the inhibition of ¹⁴C acetate incorporation into hepatic sterols, was measured after oral administration of a single dose of program compounds (Table 1). This model provided a measure of in vivo activity as well as an assessment of oral absorption. Not unexpectedly, significant increases in compound polarity often led to reduced activity in this assay (most likely due to decreased intestinal permeability leading to poor oral absorption). This acute pharmacodynamic assay served to effectively triage compounds for further testing in more extensive chronic efficacy and safety in vivo models. In general, compounds that displayed >40% inhibition at ≤ 1 mg/kg oral dose in the acute rat model were advanced into the chronic guinea pig efficacy and safety model (Table 2).

Table 2. In Vivo Guinea Pig Efficacy and Safety Data

compd	rat ED ₅₀ or % inhib at 1 mg/kg ^a	HPLC log <i>P</i> ^a	guinea pig ED ₅₀ (mg/kg) ^b	myotoxic dose in guinea pig ^c (safety window ^d)
10a	60%	2.2	90	> 100 mg/kg (>1)
10b	86%	3.14	26	< 10 mg/kg (<0.4)
12a	62%	2.3	> 90 mg/kg (30%)	> 90 mg/kg ^e (NA)
9c	64%	1.8	> 100 (31%)	> 100 mg/kg (NA)
13a	50%	1.3	> 100 (28%)	> 100 mg/kg (NA)
13b	0.067 mg/kg	2.0	> 100 (27%)	100 mg/kg (NA)
1b	0.11 mg/kg	2.16	28	> 100 mg/kg (>3.5)
atorvastatin	0.26 mg/kg	3.76	55	100 mg/kg (2.0)
rosuvastatin	0.35 mg/kg	2.4	54	100 mg/kg (1.9)
simvastatin	0.40 mg/kg	4.84	81	none (> 1.5)
pravastatin	0.68 mg/kg	2.2	> 200 (31%)	none (NA)
cerivastatin	0.09 mg/kg	4.49	1.2	0.6 mg/kg (0.25)

^a Data reproduced from Table 1 for comparison. ^b Reduction in plasma total cholesterol (TC) levels after treatment with various doses of program compounds (typically 10, 30, and 100 mg/kg) for 10 days. ED₅₀ values represent the dose (extrapolated from the dose–response curve) in which plasma TC was lowered by 50% (relative to mean value of vehicle control treatment group) at the end of the study. Values in parentheses represent the percent cholesterol lowering at the highest dose tested. Dosing of reference statins: cerivastatin 0.1, 0.3, 0.6, 1.2 mg/kg; pravastatin 50, 100, 150, 200 mg/kg; simvastatin 30, 60, 90, 125 mg/kg; rosuvastatin 10, 25, 50, 75, 100 mg/kg; atorvastatin 25, 50, 100, 150, 200, 250 mg/kg, *n* = 5 per dose group (except atorvastatin and rosuvastatin *n* = 8). ^c The lowest dose in which at least one individual animal within the treatment group exhibited a plasma CK value >2.5× the mean plasma CK value of the vehicle control group or exhibited histopathologic evidence of myofiber degeneration. ^d The ED₅₀ value for TC lowering divided by the highest dose in which no animals exhibited a plasma CK value >2.5× the mean plasma CK value of the vehicle control group. ^e Highest dose = 90 mg/kg. NA = not applicable.

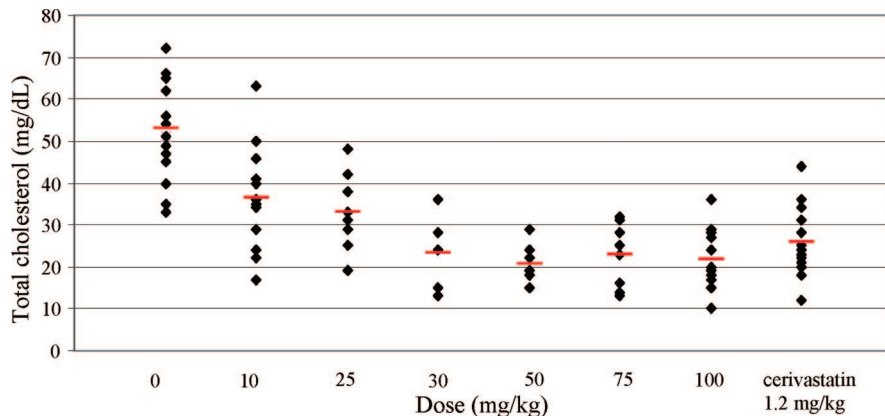
Guinea Pig Model for Efficacy and Myotoxicity. In order to best define the therapeutic window for new compounds, we conducted both efficacy and safety studies in a single animal model. We developed a 10-day efficacy and safety guinea pig model to evaluate program compounds (Table 2).³² The selection of this model was based on the ability of statins to reduce cholesterol levels in guinea pig,^{37,38} an in-house observation regarding the susceptibility of this species to statin-induced myopathy, and similarity of lipid profiles between guinea pig and human.³⁹ The utility of this model to predict efficacy and myotoxicity was demonstrated by using marketed statins with well-established clinical profiles (cerivastatin, rosuvastatin, atorvastatin, etc.).³²

In general, highly polar compounds with log *P* values ≤ 2.0, though more selective in vitro (e.g., compounds **9c**, **13a**, and **13b**), were found to exhibit modest in vivo reduction of plasma cholesterol in guinea pigs (ED₅₀ > 100 mg/kg). In contrast, more lipophilic compounds such as **10b** (HPLC log *P* = 3.14) and cerivastatin exhibited good efficacy and significantly reduced plasma TC levels. While the diminished in vivo efficacy of the more polar statins may be rationalized by reduced oral absorption as a result of attenuated intestinal permeability (caco permeability < 15 nm/s for **13b** vs 156 nm/s for **10b**), the robust pharmacodynamic response for **13b** in the acute rat model indicates that poor oral absorption was not an issue. Thus, differences in metabolism and clearance rates, perhaps species related, must also be considered. Additionally, the pharmacodynamic response in the rat model (inhibition of hepatic cholesterol synthesis) is relatively acute, whereas the lowering of plasma cholesterol in the guinea pig, as mediated by increased LDL-C uptake by the liver, represents a more chronic response. With regard to safety, as predicted by the in vitro cell selectivity data, the more lipophilic compounds were found to be myotoxic in guinea pigs (as indicated by elevated plasma CK levels and histopathology) at doses ≤ the ED₅₀ for total cholesterol (TC) reduction. The in vivo myotoxicity potential of compounds, as detected by significant elevations of CK in guinea pigs, could generally be predicted by hepatocyte/myocyte selectivity ratios of <50–60. While there were some exceptions, compounds with log *P* values of ~2.0 to 2.8 generally displayed good hepatocyte selectivity as well as good in vivo efficacy and safety. This value may correspond to an optimal balance between cellular selectiv-

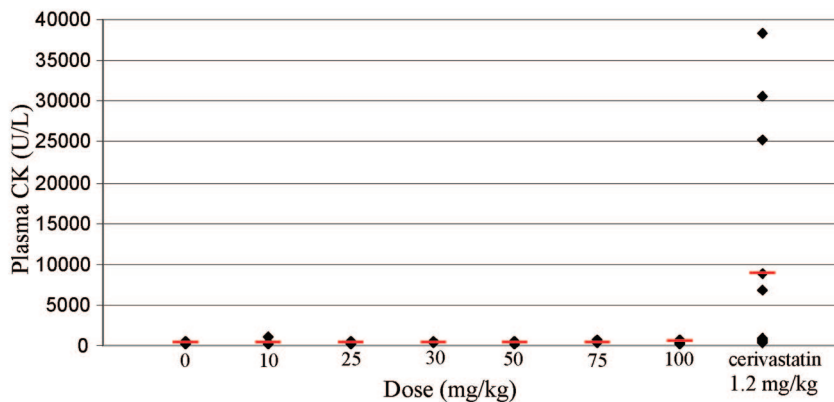
ity and intestinal permeability. The top lead triazole compound **1b**, with an HPLC log *P* value of 2.16, lowered TC in guinea pig with an ED₅₀ value of 28 mg/kg in the absence of plasma CK elevation.

The guinea pig data obtained for **1b** was compared to data obtained for multiple reference statins.³² In a direct assessment (Figure 4), the difference in safety windows of **1b** (ED₅₀ = 28 mg/kg) and cerivastatin (ED₅₀ = 1.2 mg/kg) was quite obvious. For **1b**, there were no incidences of CK elevation (>2.5 times vehicle mean) up to the 100 mg/kg dose (~3.5× the ED₅₀).⁴⁰ Thus, the myotoxic dose for **1b** is defined in this model as being >3.5× the ED₅₀ (Table 2). In contrast, treatment with cerivastatin at 1.2 mg/kg led to 50% TC lowering with 3 out of 5 animals exhibiting a >72-fold increase in plasma CK levels. Analysis by this method indicated that **1b** has a greater safety window as compared to cerivastatin (0.25×), rosuvastatin (1.9×), and atorvastatin (2.0×). Studies conducted with simvastatin (safety window >1.5×) were complicated due to poor solubility of the drug and nonlinear exposure of the compound. Thus, the safety windows for **1b** and simvastatin can not be justly compared. Pravastatin, which exhibited no myotoxicity at doses up to 200 mg/kg, was only moderately efficacious (31% TC lowering) in this model and thus does not represent a good comparator.

In addition to myotoxicity, on-target hepatotoxicity represents an important potential adverse effect of statin therapy.⁴¹ Thus, plasma levels of alanine aminotransferase (ALT) and aspartate aminotransferase (AST) were monitored during our guinea pig studies. All reference statins (with the exception of pravastatin) caused elevations of ALT and AST (>2.5× control) at doses equal to or just below their respective ED₅₀ values for TC lowering (data not shown). As a more definitive means for assessing hepatotoxicity, histopathological analyses were performed for the reference statins and **1b** (Table 3). In general, lesion severity coincided with liver enzyme elevation. For atorvastatin, rosuvastatin, and **1b**, minimal to moderate hepatocellular degeneration was observed at doses near the ED₅₀ for TC lowering. Less severe and/or a lower incidence of hepatotoxicity was noted for the other three statins tested. Of note, the histopathologic characteristics of hepatotoxicity induced by tested statins were similar, consistent with a common mechanism of action. To support this conclusion, additional in



Dose (mg/kg)	0	10	25	30	50	75	100	cerivastatin 1.2
Total cholesterol	52.8	36.4	33.1	23.2	20.5	22.8	21.6	26.0
SD	12.7	10.8	9.3	9.5	4.4	7.6	6.8	10.3
P value	-	< 0.01	< 0.01	< 0.01	< 0.01	< 0.01	< 0.01	< 0.01
% Lowering	0.0	31.1	37.3	56.1	61.2	56.9	59.1	50.8



Dose (mg/kg)	0	10	25	30	50	75	100	cerivastatin 1.2
Mean CK (U/L)	373.8	404.8	420.8	412.8	350.8	429.0	466.3	8808.2
SD	89.0	219.0	112.0	65.0	106.7	118.5	169.7	13419.1
P value	-	0.637	0.317	0.306	0.603	0.265	0.091	0.043 ^a

Figure 4. Hypolipidemic effect (top) and corresponding plasma CK levels (bottom) in guinea pigs treated with **1b** or cerivastatin (1.2 mg/kg). Combined data from two different studies: study 1, *n* = 5 at 0, 10, 30, and 100 mg/kg; study 2, *n* = 8 at 0, 10, 25, 50, 75, and 100 mg/kg. TC and CK levels (diamonds) and group means (bars) from individual animals. Data are presented as means ± SD. *P* values < 0.05 are considered significant. ^aSignificant variance between individual CK values within this treatment group precluded meaningful data assessment based on *P* value.

Table 3. Comparative Analysis of **1b** with Reference Statins for Hepatotoxicity As Determined by Liver Histopathology^a

statin	maximum cholesterol lowering or ED ₅₀ (mg/kg)	histopathology of liver (lesions incidences)
1b	28	minimal to moderate hepatocellular degeneration at 25 mg/kg (4/8); more severe at higher doses
atorvastatin	50	minimal to moderate hepatocellular degeneration at 50 mg/kg (2/5); more severe at higher doses
rosuvastatin	54	minimal to moderate hepatocellular degeneration at 50 mg/kg (4/8); more severe at higher doses
simvastatin	81	normal at all doses
pravastatin	ca. 31%	minimal hepatocellular degeneration at the highest tested dose of 200 mg/kg (1/5)
cerivastatin	1.2	normal at all doses

^a Data reported are from multiple independent studies.

Table 4. Myotoxicity of **1b** and Reference Statins in Weanling Rats As Compared to Their ED₅₀ Values for the Acute Inhibition of Hepatic Cholesterol Synthesis in Adult Rats

statin	acute adult rat ED ₅₀	myotoxic dose in weanling rats ^{a,b}	safety window ^b
atorvastatin	0.26 mg/kg	100 mg/kg	384
rosuvastatin	0.35 mg/kg	100 mg/kg	286
simvastatin	0.40 mg/kg	50 mg/kg	125
pravastatin	0.68 mg/kg	> 500 mg/kg	> 735
cerivastatin	0.09 mg/kg	< 1 mg/kg	< 11
1b	0.11 mg/kg	> 50 mg/kg	> 455

^a Weanling rats ($n = 5/\text{treatment group}$) were dosed orally once daily for 10 days; cerivastatin 1, 1.5, 2, 2.5, 3 mg/kg; pravastatin 300, 400, 500 mg/kg; simvastatin 10, 25, 50, 75 mg/kg; rosuvastatin 50, 100, 150, 200 mg/kg; atorvastatin 50, 100, 125, 150, 200 mg/kg; and compound **1b** 10, 20, 30, 40, 50 mg/kg. ^b Determination of the myotoxic dose and calculation of the safety window were as described for guinea pig in Table 2.

vivo studies were conducted in which mevalonate (a downstream product of HMGR) was coadministered with either atorvastatin (150 mg/kg) or **1b** (125 mg/kg) for 10 days (data not shown). For both compounds, mevalonate supplementation resulted in normal plasma ALT/AST levels as well as normal liver histology. Similar to conclusions derived from prior studies in rabbit,⁴² it was concluded here that the hepatotoxic effects observed in guinea pig for **1b** and atorvastatin were target based.

Weanling Rat Modeling of Myotoxicity. In order to further characterize the myotoxic potential of test statins, compound **1b**, along with the five reference statins, was evaluated in a previously described weanling rat model.⁴³ Weanling rats (~3 weeks old), perhaps due to their rapid growth, appear to be more sensitive to HMGR inhibition in the muscle, and myopathy occurs at relatively lower doses of statins as compared to the adult rat.⁴⁴ However, the myopathic signs (e.g., muscle weakness and morbidity/mortality that correlate with increases in plasma CK levels) are not age-dependent. In addition, while the lipophilic statins (e.g., simvastatin and lovastatin) have been reported to induce significant myopathy in this model, the hydrophilic pravastatin does not cause myopathy.⁴³

Animals were orally dosed once daily for 10 days. On the final day of study animals were sacrificed and assessed for myotoxicity based on plasma CK and skeletal muscle histopathology (Table 4). Due to a strong hepatic compensatory response, chronic statin treatment in rats has a relatively minimal effect on plasma TC levels.⁴⁵ Thus, the ED₅₀ values for inhibition of hepatic cholesterol synthesis derived from the acute rat model (Table 1) were used as surrogate efficacy markers for making comparisons to the respective myotoxic findings and for estimating safety margins. Clearly, there are limitations to this approach; such comparisons do not account for potential differences between adult and weanling animals, nor do they account for acute versus chronic pharmacology. Nonetheless, this approach provides a reasonable means for relating toxicity with pharmacodynamics. The calculated safety windows for the reference statins were as follows: cerivastatin (most toxic) >>> simvastatin > rosuvastatin > atorvastatin >>> pravastatin (least toxic). Similar to the guinea pig, the weanling rat was increasingly susceptible to myotoxicity when exposed to the more lipophilic compounds. Compound **1b**, with an acute rat ED₅₀ value of 0.11 mg/kg, was dosed to weanling rats at 10, 20, 30, 40, and 50 mg/kg, corresponding to approximate multiples of 100-, 200-, 300-, 400-, and 500-fold the acute ED₅₀ value, respectively. None of the animals dosed with **1b** showed signs of myopathy based on plasma CK levels, which were comparable to the vehicle-treated group. Therefore, the myotoxic dose for **1b** is >50 mg/kg, which corresponds to >455-fold

the acute ED₅₀ (0.11 mg/kg) for acute cholesterol synthesis inhibition. For comparison, the myotoxic doses for reference statins in weanling rats were 100 mg/kg each for atorvastatin and rosuvastatin, 50 mg/kg for simvastatin, and <1 mg/kg for cerivastatin.

Summary

In Vitro Data. Compared to the reference statins (Tables 1, 5), compound **1b** (IC₅₀ = 1.4 nM) was among the most potent in the rat enzyme assay. The mean IC₅₀ values for **1b** for inhibition of cholesterol synthesis in freshly isolated rat hepatocytes and L6 myocytes were 3.95 and 995 nM, respectively. Compound **1b** was also determined to be similarly potent in human primary hepatocytes, with a calculated IC₅₀ value of 1.7 nM. In rat hepatocytes, the potency of **1b** was similar to that of cerivastatin (2.3 nM), atorvastatin (2.5 nM), and simvastatin (6.2 nM), but lower than rosuvastatin (0.6 nM), and several-fold higher than pravastatin (29 nM). With the exception of pravastatin (IC₅₀ = 1519 nM), **1b** was the least potent of the reference statins in the L6 myocytes. Compound **1b** exhibited a high L6 myocyte/hepatocyte IC₅₀ selectivity ratio (252×), which was superior to both the polar statins rosuvastatin (108×) and pravastatin (52×) as well as the less polar statins simvastatin (4×) and atorvastatin (31×).⁴⁶ In agreement with its increased propensity for myotoxicity in humans, cerivastatin, the least polar statin of the set, exhibited the lowest selectivity ratio (0.7×).

In Vivo Data. In the guinea pig model (Tables 2, 5), **1b** displayed an ED₅₀ = 28 mg/kg (superior to atorvastatin and rosuvastatin) with maximum efficacy in the superstatin range (~60% total cholesterol lowering) with no CK elevation incidences (>2.5× vehicle mean) at doses up to 3.5× the ED₅₀ for TC lowering (better than atorvastatin). In the weanling rat model (Tables 4, 5), **1b** did not result in a CK increase (>2.5× vehicle mean) at doses >455× the ED₅₀ for acute inhibition of cholesterol synthesis. **1b** induces hepatotoxicity in the guinea pig in a manner that is similar to other marketed statins with respect to both frequency and pathology, and the toxicity can be completely ameliorated with the coadministration of mevalonate.

Pharmacokinetic Data. Given that the liver is the target organ for statin-mediated LDL-C lowering, and because increased systemic exposure could lead to enhanced myotoxicity, adequate oral absorption combined with efficient liver extraction represent desirable pharmacokinetic properties for this class of compounds. The oral bioavailability (AUC_{PO}/AUC_{IV}) of **1b** was determined in the guinea pig (41%), rat (2.8%), dog (11%), and monkey (ca. 1%). Oral absorption (AUC_{PO}/AUC_{IP}) was determined in the guinea pig (64%) and rat (20%). These results indicate moderate to highly efficient liver extraction in our preclinical models (35% and 86% in guinea pig and rat, respectively). A comparative analysis of drug levels in blood (portal vein, hepatic vein, and inguinal vein), liver, and bile samples obtained from an orally dosed monkey revealed 98% hepatic extraction. High concentrations of drug in liver and bile suggest that oral absorption was adequate in monkey. The animal pharmacokinetic data for **1b** compare favorably with the human gut absorption and liver extraction data reported for atorvastatin (30% and >70%, respectively) and rosuvastatin (20% and 90%, respectively).⁴⁷

Additional Profiling. Compound **1b** is neither a substrate for nor an inhibitor of cytochrome P450 enzymes (CYP1A2, 2C8, 2C9, 2C19, 2D6, and 3A4) and thus displays a low potential for drug–drug interactions. In addition, **1b** is not an

Table 5. Summary of in Vitro and in Vivo Profiling Data for **1b** As Compared to Reference Statins

		1b	atorvastatin	rosuvastatin	simvastatin	pravastatin	cerivastatin
log <i>P</i> (HPLC)		2.2	3.8	2.4	4.8	2.2	4.5
in vitro data	rat enzyme IC ₅₀ (nM)	1.4	6.2	3.1	4.3	31.6	9.8
	rat hepatocyte/rat myocyte IC ₅₀ (nM)	3.95/995	2.5/78	0.6/65	6.2/27	29/1519	2.3/1.7
	cell selectivity	252	31	108	4.4	52	0.7
guinea pig data	ED ₅₀ (mg/kg)	28	50	54	81	NA (31%)	1.2
	myotoxic dose (CK > 2.5×)	none	100 mg/kg	100 mg/kg	none	none	0.3 mg/kg
	myotoxic dose (CK > 10×)	none	none	none	none	none	0.6 mg/kg
	myotoxic dose (CK > 2.5×) relative to ED ₅₀	> 3.5×	2.0×	1.9×	> 1.5×	NA	0.25×
	CK > 10000 U/L	none	none	none	none	none	yes
rat data	acute ED ₅₀ (mg/kg)	0.11	0.26	0.35	0.40	0.68	0.09
	myotoxic dose (CK > 2.5) in WR (mg/kg)	> 50	100	100	50	> 500	< 1
	myotoxic dose (CK > 2.5) in WR (mg/kg) as related to ED ₅₀	> 455×	384×	286×	125×	> 735×	< 11×

inducer of CYP3A4 and is neither a P-gp substrate nor an inhibitor. There was no evidence of significant receptor binding or enzyme inhibition in a broad receptor screening panel. Ames and in vitro micronucleus assays were negative, suggesting a low potential for mutagenicity. Furthermore, **1b** displayed no significant in vitro or in vivo cardiovascular liabilities.

Clinical Data. Compound **1b** was dosed to humans in a placebo-controlled, ascending single-dose study to evaluate the safety, pharmacokinetics, and pharmacodynamics in healthy subjects.⁴⁸ Single oral doses of **1b** in the range 0.25 to 120 mg were safe and well tolerated. Indicative of its potential as a statin with an excellent efficacy and safety (myotoxicity) profile, compound **1b** produced dose-dependent reductions in plasma mevalonic acid with minimal systemic exposure. As an example, at the 10 mg dose (*N* = 6), compound **1b** generated a geometric mean *C*_{max} of 4.72 (33% CV) ng/mL and a mean percent change (±SD) from baseline in plasma mevalonic acid AUC_(0–24 h) of –48.19 (±8.16). In comparison, rosuvastatin, when dosed (10 mg each morning) to healthy adult volunteers (*n* = 21) for 14 days in an open-label clinical trial, generated a geometric mean *C*_{max} of 4.58 ng/mL and a mean percent change from baseline in plasma mevalonic acid AUC_(0–24 h) of –29.9.⁴⁹

In conclusion, compound **1b** met or exceeded our initial criteria for clinical development by generating an excellent profile both in vitro and in the guinea pig and rat models. These data, combined with results from additional toxicity studies and early clinical trials, provide evidence that compound **1b** has the potential to be a highly efficacious statin with a reduced propensity for myotoxicity, leading to an overall excellent risk–benefit profile.

Experimental Section

General Procedures. All reagents and solvents purchased from commercial resources were used without further purification. Silica gel 60 (Merck) was used for flash chromatography, and silica gel 60 F254 (Merck) plates were used for thin-layer chromatography (TLC). TLC spots were examined under UV light at 254 nm. Analytical HPLC analyses were performed under the following conditions. System A: Phenomenex Prime S5 C18 4.6 × 50 mm column/water–MeOH–H₃PO₄ 90:10:0.2 to 10:90:0.2 gradient over 4 min at 4 mL/min with 1 min hold at the end of the gradient. System B (used with LC/MS): Phenomenex S5 C18 4.6 × 30 mm column/water–MeOH–TFA 90:10:0.1 to 10:90:0.1 gradient over 2 min at 5 mL/min with 1 min hold at the end of the gradient. System C (used with LC/MS): YMC S5 C18 4.6 × 50 mm column/water–MeOH–TFA 90:10:0.1 to 10:90:0.1 gradient over 4 min at 4 mL/min with 1 min hold at the end of the gradient. System D: YMC S5 C18 4.6 × 50 mm column/water–MeOH–H₃PO₄ 90:10:0.2 to 10:90:0.2 gradient over 4 min at 4 mL/min with 1 min hold at the end of the gradient. NMR data were obtained using a Bruker or JEOL 400 or 500 MHz spectrometer. All final compounds were of ≥95% purity by the LC/MS and analytical HPLC systems

and were characterized by NMR analysis. Samples prepared for in vivo studies were of ≥98% purity.

(4-(4-Fluorophenyl)-6-isopropyl-2-(methylsulfonyl)pyrimidin-5-yl)methanol (3). A solution of DIBAL in methylene chloride (1 M, 25 mL, 25 mmol) was added over 5 min to a stirred solution of ethyl 4-(4-fluorophenyl)-6-isopropyl-2-(methylsulfonyl)pyrimidine-5-carboxylate²⁸ (3.7 g, 10.1 mmol) in toluene (100 mL) at –78 °C. The reaction mixture was stirred at –78 °C for 30 min followed by a slow addition of saturated ammonium chloride. The mixture was stirred at RT for 30 min, and the organic layer was dried (MgSO₄) and concentrated. The crude product was subjected to flash chromatography (silica gel/hexanes–ethyl acetate 80:20 to 20:80) to give the title compound **3** as a white solid (2.0 g, 61%): ¹H NMR (400 MHz, CDCl₃) δ 7.81 (2 H, dd, *J* = 5.3, 8.6 Hz), 7.16 (2 H, t, *J* = 8.6 Hz), 4.72 (2 H, s), 3.64 (1 H, m), 3.39 (3 H, s), 2.69 (1 H, br s), 1.36 (6 H, d, *J* = 6.7 Hz); MS (ESI) *m/z* 325 (M + H)⁺; analytical HPLC (system A) *t*_R = 2.89 min, (system B) *t*_R = 2.29 min.

4-(4-Fluorophenyl)-6-isopropyl-2-(methylsulfonyl)pyrimidine-5-carbaldehyde (4). To a solution of compound **3** (2.0 g, 6.2 mmol) in ethyl acetate (20 mL) were added potassium bromide (73 mg, 0.61 mmol) and TEMPO free radical (10 mg, 0.064 mmol), and the reaction mixture was cooled to 0 °C. A solution of buffered commercial bleach (0.824 M, adjusted to pH 9.4 with solid sodium bicarbonate, 15 mL) was then added over 0.5 h while maintaining the reaction temperature between 5 and –5 °C. The mixture was then washed sequentially with water, 5% sodium thiosulfate, 1 N NaOH, and brine. The organic phase was dried (MgSO₄) and concentrated, and the crude aldehyde **4** thus obtained (1.98 g, 100%, unpurified) was used as such in the next step. ¹H NMR (400 MHz, CDCl₃) δ 10.05 (1 H, s), 7.69 (2 H, dd, *J* = 5.2, 8.8 Hz), 7.26 (2 H, t, *J* = 8.5 Hz), 3.88 (1 H, m), 3.44 (3 H, s), 1.37 (6 H, d, *J* = 6.8 Hz); LC/MS and LC showed a mixture of the aldehyde and the corresponding methanol-hemiacetal; MS (ESI) *m/z* 323 (M + H)⁺ and 355 (M + MeOH + H)⁺; analytical HPLC (system A) *t*_R = 2.36, 3.46 min.

tert-Butyl 2-((4R,6S)-6-((E)-2-(4-(4-fluorophenyl)-6-isopropyl-2-(methylsulfonyl)pyrimidin-5-yl)vinyl)-2,2-dimethyl-1,3-dioxan-4-yl)acetate (5). A solution of lithium bis(trimethylsilyl)amide (1 M in THF, 667 mL, 0.667 mol) was added with stirring to a solution of the aldehyde **4** from above (118 g, 0.365 mol) and compound **6**³¹ (165 g, 0.365 mol) in THF (1.5 L) at –60 °C over 15 min. The mixture was allowed to come to RT, washed with saturated sodium bicarbonate solution, dried (MgSO₄), and concentrated. The crude product was flash chromatographed using a short column of silica gel (hexane–ethyl acetate 100:0 to 50:50 gradient) to give the title compound **5** as a white solid (200 g, 99.6%): ¹H NMR (400 MHz, CDCl₃) δ 7.70 (2 H, dd, *J* = 8.8, 5.3 Hz), 7.11 (2 H, t, *J* = 8.6 Hz), 6.61 (1 H, dd, *J* = 16.1, 1.5 Hz), 5.60 (1 H, dd, *J* = 16.1, 4.5 Hz), 4.29 (1 H, m), 4.46 (1 H, m), 3.46 (1 H, m), 3.40 (3 H, s), 2.45 (1 H, dd, *J* = 15.1, 7.1 Hz), 2.30 (1 H, dd, *J* = 15.4, 6.3 Hz), 2.3 Hz), 1.40–1.55 (17 H, m, 3 singlets overlapping a multiplet), 1.32 (6 H, d, *J* = 6.8 Hz); MS (ESI) *m/z* 549 (M + H)⁺; analytical HPLC purity (system C) 88%, *t*_R = 3.58 min.

Sodium (3*R*,5*S*,*E*)-7-(4-(4-fluorophenyl)-6-isopropyl-2-(methyl(1-methyl-1*H*-1,2,4-triazol-5-yl)amino)pyrimidin-5-yl)-3,5-dihydroxyhept-6-enoate (1b). A solution of lithium bis(trimethylsilyl)amide (1 M in THF, 146 mL, 146 mmol) was added dropwise at -60°C to a stirred solution of 1-methyl-1*H*-1,2,4-triazol-5-amine⁵⁰ (14.3 g, 145.9 mmol) and compound **5** (33 g, 60.2 mmol) in 300 mL of DMF. The reaction mixture was stirred at -60°C for 30 min followed by the addition of methyl iodide (68 g, 479 mmol). The mixture was allowed to come to RT, stirred for 30 min, and partitioned between ethyl acetate and saturated sodium bicarbonate solution. The organic layer was dried (MgSO_4) and concentrated, and the residue was subjected to flash chromatography (silica gel/hexanes—ethyl acetate 100:0 to 50:50 gradient) to afford *tert*-butyl 2-((4*R*,6*S*)-6-((*E*)-2-(4-(4-fluorophenyl)-6-isopropyl-2-(methyl(1-methyl-1*H*-1,2,4-triazol-5-yl)amino)pyrimidin-5-yl)vinyl)-2,2-dimethyl-1,3-dioxan-4-yl)acetate (**7b**) as a pale gummy solid (25 g, 72%): $^1\text{H NMR}$ (400 MHz, CDCl_3) δ 7.86 (1 H, s), 7.56 (2 H, dd, $J = 9.07, 5.54$ Hz), 7.05 (2 H, t, $J = 8.81$ Hz), 6.47 (1 H, dd, $J = 16.12, 1.01$ Hz), 5.40 (1 H, dd, $J = 16.37, 5.79$ Hz), 4.40 (1 H, dd, $J = 10.58, 5.54$ Hz), 3.67 (3 H, s), 4.27 (1 H, m), 3.29 (1 H, m), 3.58 (3 H, s), 2.44 (1 H, dd, $J = 15.11, 6.55$ Hz), 2.29 (1 H, dd, $J = 15.36, 6.30$ Hz), 1.48 (3 H, s), 1.50 (2 H, m), 1.46 (9 H, s), 1.39 (3 H, s), 1.14 (6 H, t, $J = 6.55$ Hz); MS (ESI) m/z 581 ($\text{M} + \text{H}^+$); analytical HPLC (system D) $t_R = 4.59$ min.

Compound **7b** was dissolved in THF (75 mL) and treated with 6 N HCl (22 mL). After 15 min, the reaction mixture was made basic by the addition of 6 N NaOH (30 mL) followed by the addition of methanol (5 mL). The mixture was stirred at RT for 15 min and concentrated, and the residue was subjected to reversed-phase chromatography (C18/water—MeOH 100:0 to 50:50 gradient) to afford the title compound as a white solid (11.1 g, 36% yield from the sulfone **5**): $^1\text{H NMR}$ (500 MHz, CD_3OD) δ 7.91 (1 H, s), 7.61 (2 H, dd, $J = 8.3, 5.5$ Hz), 7.14 (2 H, t, $J = 8.8$ Hz), 6.54 (1 H, d, $J = 16.5$ Hz), 5.48 (1 H, dd, $J = 16.2, 6.3$ Hz), 4.26–4.39 (1 H, m), 3.83–3.97 (1 H, m), 3.67 (3 H, s), 3.53 (3 H, s), 3.34–3.49 (1 H, m), 2.17–2.37 (2 H, m), 1.56–1.70 (1 H, m), 1.39–1.54 (1 H, m), 1.16 (3 H, s), 1.15 (3 H, s); MS (ESI) m/z 525 ($\text{M} + \text{H}^+$). Anal. ($\text{C}_{24}\text{H}_{28}\text{FN}_6\text{NaO}_4 \cdot 1.59\text{H}_2\text{O}$) C, H, N.

Sodium (3*R*,5*S*,*E*)-7-(4-(4-fluorophenyl)-6-isopropyl-2-(1-methyl-1*H*-1,2,4-triazol-5-ylamino)pyrimidin-5-yl)-3,5-dihydroxyhept-6-enoate (1a). This compound was prepared in a manner similar to that described for the synthesis of compound **1b** except that the step involving alkylation with MeI was omitted. $^1\text{H NMR}$ (500 MHz, CD_3OD) δ 7.84 (s, 1 H), 7.61 (dd, $J = 8.6, 5.5$ Hz, 2 H), 7.14 (t, $J = 8.9$ Hz, 2 H), 6.54 (d, $J = 15.9$ Hz, 1 H), 5.48 (dd, $J = 16.2, 6.4$ Hz, 1 H), 4.32 (q, $J = 6.7$ Hz, 1 H), 3.87–3.95 (m, 1 H), 3.38–3.48 (m, 1 H), 3.76 (s, 3 H), 2.23 (dd, 1 H), 2.31 (dd, 1 H), 1.58–1.68 (m, 1 H), 1.43–1.51 (m, 1 H), 1.20 (d, $J = 6.7$ Hz, 6 H); MS (ESI) m/z 471 ($\text{M} + \text{H}^+$); analytical HPLC (system B) $t_R = 1.17$ min.

Sodium (3*R*,5*S*,*E*)-7-(4-(4-fluorophenyl)-6-isopropyl-2-(*N*-(1-methyl-1*H*-1,2,4-triazol-5-yl)methylsulfonamido)pyrimidin-5-yl)-3,5-dihydroxyhept-6-enoate (1c). This compound was prepared in a manner similar to that described for the synthesis of compound **1b** except that MeI was substituted with methanesulfonyl chloride. $^1\text{H NMR}$ (400 MHz, CD_3OD) δ 8.04 (1 H, s), 7.67 (2 H, dd, $J = 8.3, 5.5$ Hz), 7.16 (2 H, t, $J = 9.0$ Hz), 6.60 (1 H, d, $J = 17.0$ Hz), 5.60 (1 H, dd, $J = 16.2, 6.0$ Hz), 4.40–4.25 (1 H, m), 3.90 (4 H, br s), 3.75 (3 H, s), 3.55–3.47 (1 H, m), 2.34 (1 H, dd, $J = 15.5, 4.9$ Hz), 2.25 (1 H, dd, $J = 15.5, 7.9$ Hz), 1.70–1.64 (1 H, m), 1.58–1.50 (1 H, m), 1.22 (3 H, d, $J = 1.58$ Hz), 1.20 (3 H, d, $J = 1.58$ Hz); MS (ESI) m/z 549 ($\text{M} + \text{H}^+$); analytical HPLC (system B) $t_R = 1.38$ min.

Sodium (3*R*,5*S*,*E*)-7-(4-(4-fluorophenyl)-6-isopropyl-2-(5-phenyl-1,2,4-thiadiazol-3-ylamino)pyrimidin-5-yl)-3,5-dihydroxyhept-6-enoate (8a). This compound was prepared from compound **5** and 5-phenyl-1,2,4-thiadiazol-3-amine as described for compound **1a**. $^1\text{H NMR}$ (400 MHz, CD_3OD) δ 8.04 (2 H, dd, $J = 8.1, 1.5$ Hz), 7.77 (2 H, dd, $J = 9.1, 5.5$ Hz), 7.53–7.60 (3 H, m), 7.18 (2 H, t, $J = 8.8$ Hz), 6.62 (1 H, dd, $J = 16.1, 1.0$ Hz), 5.54 (1 H, dd, $J = 16.1, 6.0$ Hz), 4.36 (1 H, q, $J = 6.0$ Hz), 3.91–3.98 (1 H, m), 3.43–3.57 (1 H,

m), 2.34 (1 H, dd, $J = 19.6, 4.5$ Hz), 2.25 (1 H, dd, $J = 15.1, 7.6$ Hz), 1.61–1.71 (1 H, m), 1.47–1.55 (1 H, m), 1.32 (6 H, d, $J = 6.5$ Hz); MS (ESI) m/z 550 ($\text{M} + \text{H}^+$); analytical HPLC (system B) $t_R = 1.71$ min.

Sodium (3*R*,5*S*,*E*)-7-(4-(4-fluorophenyl)-6-isopropyl-2-(isoxazol-3-ylamino)pyrimidin-5-yl)-3,5-dihydroxyhept-6-enoate (9a). This compound was prepared from compound **5** and isoxazol-3-amine as described for compound **1a**. $^1\text{H NMR}$ (400 MHz, CD_3OD) δ 8.46 (1 H, d, $J = 1.5$ Hz), 7.67 (2 H, dd, $J = 9.1, 5.5$ Hz), 7.26 (1 H, d, $J = 1.5$ Hz), 7.17 (2 H, t, $J = 8.8$ Hz), 6.56 (1 H, dd, $J = 16.1, 1.0$ Hz), 5.49 (1 H, dd, $J = 16.1, 6.5$ Hz), 4.33 (1 H, q, $J = 6.5$ Hz), 3.79–4.12 (1 H, m), 3.34–3.65 (1 H, m), 2.32 (3 H, dd, $J = 15.1, 4.5$ Hz), 2.24 (1 H, dd, $J = 15.1, 8.1$ Hz), 1.57–1.70 (1 H, m), 1.40–1.53 (1 H, m), 1.29 (6 H, d, $J = 6.5$ Hz); MS (ESI) m/z 457 ($\text{M} + \text{H}^+$); analytical HPLC (system A) $t_R = 3.33$ min, (system B) $t_R = 1.52$ min.

Sodium (3*R*,5*S*,*E*)-7-(4-(4-fluorophenyl)-6-isopropyl-2-(isoxazol-3-yl(methylamino)pyrimidin-5-yl)-3,5-dihydroxyhept-6-enoate (9b). This compound was prepared from compound **5** and isoxazol-3-amine as described for compound **1b**. $^1\text{H NMR}$ (400 MHz, D_2O) δ 8.30 (1 H, d, $J = 2.0$ Hz), 7.43 (2 H, dd, $J = 8.6, 5.5$ Hz), 7.09 (2 H, t, $J = 8.8$ Hz), 6.99 (1 H, d, $J = 2.0$ Hz), 6.51 (1 H, d, $J = 15.6$ Hz), 5.34 (1 H, dd, $J = 16.1, 7.1$ Hz), 4.22 (1 H, q, $J = 6.5$ Hz), 3.58–4.07 (1 H, m), 3.47 (3 H, s), 3.24–3.38 (1 H, m), 2.05–2.28 (2 H, m), 1.42–1.64 (1 H, m), 1.24–1.47 (1 H, m), 1.14 (3 H, d, $J = 6.5$ Hz), 1.15 (3 H, d, $J = 7.1$ Hz); MS (ESI) m/z 471 ($\text{M} + \text{H}^+$); analytical HPLC (system A) $t_R = 3.80$ min, (system B) $t_R = 1.88$ min.

Sodium (3*R*,5*S*,*E*)-7-(4-(4-fluorophenyl)-6-isopropyl-2-(*N*-(isoxazol-3-yl)methylsulfonamido)pyrimidin-5-yl)-3,5-dihydroxyhept-6-enoate (9c). This compound was prepared from compound **5** and isoxazol-3-amine as described for compound **1c**. $^1\text{H NMR}$ (400 MHz, CD_3OD) δ 8.67 (1 H, d, $J = 1.5$ Hz), 7.57 (2 H, dd, $J = 8.8, 5.3$ Hz), 7.03–7.11 (2 H, m), 6.68 (1 H, d, $J = 2.0$ Hz), 6.52 (1 H, d, $J = 16.1$ Hz), 5.52 (1 H, dd, $J = 16.1, 6.0$ Hz), 4.07–4.33 (1 H, m), 3.75–3.90 (1 H, m), 3.60 (3 H, s), 3.23–3.46 (1 H, m), 1.93–2.36 (2 H, m), 1.48–1.67 (1 H, m), 1.38–1.47 (1 H, m), 1.12 (6 H, d, $J = 7.1$ Hz); MS (ESI) m/z 535 ($\text{M} + \text{H}^+$); analytical HPLC (system A) $t_R = 3.11$ min, (system B) $t_R = 0.95$ min. Anal. ($\text{C}_{24}\text{H}_{26}\text{FN}_4\text{NaO}_7\text{S} \cdot 2.1\text{H}_2\text{O}$) C, H, N, F, Na, S.

Sodium (3*R*,5*S*,*E*)-7-(4-(4-fluorophenyl)-6-isopropyl-2-(1-methyl-1*H*-pyrazol-5-ylamino)pyrimidin-5-yl)-3,5-dihydroxyhept-6-enoate (10a). This compound was prepared from compound **5** and 1-methyl-1*H*-pyrazol-5-amine as described for compound **1a**. $^1\text{H NMR}$ (400 MHz, CD_3OD) δ 7.62 (2 H, dd, $J = 9.1, 5.5$ Hz), 7.38 (1 H, d, $J = 2.0$ Hz), 7.15 (2 H, t, $J = 8.8$ Hz), 6.54 (1 H, dd, $J = 16.1, 1.5$ Hz), 6.39 (1 H, d, $J = 2.0$ Hz), 5.46 (1 H, dd, $J = 16.1, 6.0$ Hz), 4.31 (1 H, q, $J = 6.4$ Hz), 3.81–4.13 (1 H, m), 3.76 (3 H, s), 3.34–3.54 (1 H, m), 2.31 (1 H, dd, $J = 15.1, 5.0$ Hz), 2.22 (1 H, dd, $J = 15.1, 8.1$ Hz), 1.57–1.71 (1 H, m), 1.32–1.56 (1 H, m), 1.23 (6 H, d, $J = 6.5$ Hz); MS (ESI) m/z 470 ($\text{M} + \text{H}^+$); analytical HPLC (system A) $t_R = 3.21$ min, (system B) $t_R = 1.44$ min.

Sodium (3*R*,5*S*,*E*)-7-(4-(4-fluorophenyl)-6-isopropyl-2-(methyl(1-methyl-1*H*-pyrazol-5-yl)amino)pyrimidin-5-yl)-3,5-dihydroxyhept-6-enoate (10b). This compound was prepared from compound **5** and 1-methyl-1*H*-pyrazol-5-amine as described for compound **1b**. $^1\text{H NMR}$ (400 MHz, CD_3OD) δ 7.59 (2 H, dd, $J = 8.6, 5.5$ Hz), 7.47 (1 H, d, $J = 2.0$ Hz), 7.12 (2 H, t, $J = 8.8$ Hz), 6.52 (1 H, d, $J = 16.1$ Hz), 6.16 (1 H, d, $J = 2.0$ Hz), 5.44 (1 H, dd, $J = 16.1, 6.6$ Hz), 4.30 (1 H, q, $J = 6.4$ Hz), 3.87–3.93 (1 H, m), 3.63 (3 H, s), 3.48 (3 H, s), 3.34–3.43 (1 H, m), 2.18–2.34 (2 H, m), 1.57–1.67 (1 H, m), 1.42–1.51 (1 H, m), 1.14 (6 H, d, $J = 6.6$ Hz); MS (ESI) m/z 484 ($\text{M} + \text{H}^+$); analytical HPLC (system A) $t_R = 3.65$ min, (system B) $t_R = 1.67$ min. Anal. ($\text{C}_{25}\text{H}_{29}\text{FN}_5\text{NaO}_4 \cdot 1.0\text{H}_2\text{O}$) C, H, N, F, Na.

Sodium (3*R*,5*S*,*E*)-7-(4-(4-fluorophenyl)-6-isopropyl-2-(*N*-(1-methyl-1*H*-pyrazol-5-yl)methylsulfonamido)pyrimidin-5-yl)-3,5-dihydroxyhept-6-enoate (10c). This compound was prepared from compound **5** and 1-methyl-1*H*-pyrazol-5-amine as described for compound **1c**. $^1\text{H NMR}$ (400 MHz, CD_3OD) δ 7.66 (2 H, dd, $J = 8.7, 5.4$ Hz), 7.53 (1 H, d, $J = 2.0$ Hz), 7.16 (2 H, t, $J = 8.8$ Hz), 6.59 (1 H, d, $J = 16.2$ Hz), 6.36 (1 H, d, $J = 2.0$ Hz), 5.60 (1 H,

dd, $J = 16.0, 6.6$ Hz), 4.35 (1 H, q, $J = 6.4$ Hz), 3.85–3.93 (1 H, m), 3.71 (3 H, s), 3.31 (3 H, s), 3.51–3.44 (1 H, m), 2.32 (1 H, dd, $J = 15.0, 5.0$ Hz), 2.25 (1 H, dd, $J = 15.0, 8.0$ Hz), 1.63–1.70 (1 H, m), 1.47–1.55 (1 H, m), 1.19 (6 H, d, $J = 6.7$ Hz); MS (ESI) m/z 548 (M + H)⁺; analytical HPLC (system B) $t_R = 1.42$ min.

Sodium (3R,5S,E)-7-(2-(3-tert-butyl-1-methyl-1H-pyrazol-5-ylamino)-4-(4-fluorophenyl)-6-isopropylpyrimidin-5-yl)-3,5-dihydroxyhept-6-enoate (11a). This compound was prepared from compound **5** and 3-tert-butyl-1-methyl-1H-pyrazol-5-amine as described for compound **1a**. ¹H NMR (400 MHz, CD₃OD) δ 7.63 (2 H, dd, $J = 8.8, 5.3$ Hz), 7.15 (2 H, t, $J = 8.6$ Hz), 6.54 (1 H, d, $J = 15.6$ Hz), 6.31 (1 H, s), 5.46 (1 H, dd, $J = 16.1, 6.5$ Hz), 4.32 (1 H, q, $J = 6.5$ Hz), 3.83–4.00 (1 H, m), 3.71 (3 H, s), 3.36–3.51 (1 H, m), 2.31 (1 H, dd, $J = 15.1, 4.5$ Hz), 2.23 (1 H, dd, $J = 15.6, 7.6$ Hz), 1.54–1.73 (1 H, m), 1.40–1.54 (1 H, m), 1.29 (9 H, s), 1.24 (6 H, d, $J = 6.5$ Hz); MS (ESI) m/z 526 (M + H)⁺; analytical HPLC (system C) $t_R = 2.92$ min.

Sodium (3R,5S,E)-7-(4-(4-fluorophenyl)-6-isopropyl-2-(1-methyl-1H-pyrazol-3-ylamino)pyrimidin-5-yl)-3,5-dihydroxyhept-6-enoate (12a). This compound was prepared from compound **5** and 1-methyl-1H-pyrazol-3-amine as described for compound **1a**. ¹H NMR (400 MHz, CD₃OD) δ 7.64 (2 H, dd, $J = 8.6, 5.5$ Hz), 7.43 (1 H, d, $J = 2.5$ Hz), 7.16 (2 H, t, $J = 8.8$ Hz), 6.80 (1 H, d, $J = 2.5$ Hz), 6.53 (1 H, dd, $J = 16.1, 1.0$ Hz), 5.45 (1 H, dd, $J = 15.9, 6.3$ Hz), 4.31 (1 H, q, $J = 6.5$ Hz), 3.82–4.04 (1 H, m), 3.78 (3 H, s), 3.37–3.52 (1 H, m), 2.32 (1 H, dd, $J = 15.6, 5.0$ Hz), 2.23 (1 H, dd, $J = 15.1, 7.6$ Hz), 1.53–1.74 (1 H, m), 1.35–1.55 (1 H, m), 1.28 (6 H, d, $J = 7.1$ Hz); MS (ESI) m/z 470 (M + H)⁺; analytical HPLC (system C) $t_R = 2.57$ min, (system B) $t_R = 1.46$ min.

Sodium (3R,5S,E)-7-(4-(4-fluorophenyl)-6-isopropyl-2-(methyl-1-methyl-1H-pyrazol-3-yl)amino)pyrimidin-5-yl)-3,5-dihydroxyhept-6-enoate (12b). This compound was prepared from compound **5** and 1-methyl-1H-pyrazol-3-amine as described for compound **1b**. ¹H NMR (400 MHz, CD₃OD) δ 7.65 (2 H, dd, $J = 8.8, 5.5$ Hz), 6.35 (1 H, d, $J = 2.2$ Hz), 7.15 (2 H, t, $J = 8.9$ Hz), 6.75 (1 H, d, $J = 2.2$ Hz), 6.53 (1 H, d, $J = 16.0$ Hz), 5.43 (1 H, dd, $J = 16.0, 6.0$ Hz), 4.33 (1 H, q, $J = 6.0$ Hz), 3.95–3.87 (1 H, m), 3.83 (3 H, s), 3.64 (3 H, s), 3.35–3.49 (1 H, m), 2.33 (1 H, dd, $J = 16.0, 5.0$ Hz), 2.25 (1 H, dd, $J = 16.0, 7.5$ Hz), 1.56–1.68 (1 H, m), 1.36–1.48 (1 H, m), 1.26 (6 H, d, $J = 6.7$); MS (ESI) m/z 484 (M + H)⁺; analytical HPLC (system B) $t_R = 1.36$ min.

Sodium (3R,5S,E)-7-(4-(4-fluorophenyl)-6-isopropyl-2-(N-(1-methyl-1H-pyrazol-3-yl)methylsulfonamido)pyrimidin-5-yl)-3,5-dihydroxyhept-6-enoate (12c). This compound was prepared from compound **5** and 1-methyl-1H-pyrazol-3-amine as described for compound **1c**. ¹H NMR (400 MHz, CD₃OD) δ 7.58–7.65 (3 H, m), 7.14 (2 H, t, $J = 8.8$ Hz), 6.60 (1 H, d, $J = 16.0$ Hz), 6.39 (1 H, d, $J = 2.0$ Hz), 5.55 (1 H, dd, $J = 16.0, 6.0$ Hz), 4.34 (1 H, q, $J = 6.0$ Hz), 3.90–3.98 (1 H, m), 3.88 (3 H, s), 3.65 (3 H, s), 3.43–3.50 (1 H, m), 2.32 (1 H, dd, $J = 16.0, 5.0$ Hz), 2.24 (1 H, dd, $J = 16.0, 7.5$ Hz), 1.57–1.66 (1 H, m), 1.46–1.54 (1 H, m), 1.21 (6 H, d, $J = 6.6$ Hz); MS (ESI) m/z 548 (M + H)⁺; analytical HPLC (system B) $t_R = 1.30$ min.

Sodium (3R,5S,E)-7-(4-(4-fluorophenyl)-6-isopropyl-2-(1-methyl-1H-tetrazol-5-ylamino)pyrimidin-5-yl)-3,5-dihydroxyhept-6-enoate (13a). This compound was prepared from compound **5** and 1-methyl-1H-tetrazol-5-amine as described for compound **1a**. ¹H NMR (400 MHz, CD₃OD) δ 7.63 (2 H, dd, $J = 8.6, 5.5$ Hz), 7.15 (2 H, t, $J = 8.8$ Hz), 6.55 (1 H, dd, $J = 16.1, 1.0$ Hz), 5.50 (1 H, dd, $J = 16.1, 6.0$ Hz), 4.32 (1 H, q, $J = 6.5$ Hz), 3.94 (3 H, s), 3.85–3.93 (1 H, m), 3.37–3.51 (1 H, m), 2.31 (1 H, dd, $J = 15.1, 5.0$ Hz), 2.23 (1 H, dd, $J = 15.1, 7.6$ Hz), 1.55–1.68 (1 H, m), 1.34–1.52 (1 H, m), 1.21 (6 H, d, $J = 6.5$ Hz); MS (ESI) m/z 472 (M + H)⁺; analytical HPLC (system B) $t_R = 1.27$ min. Anal. (C₂₁H₂₆FN₇NaO₄·1.60H₂O) C, H, N, F, Na.

Sodium (3R,5S,E)-7-(4-(4-fluorophenyl)-6-isopropyl-2-(methyl-1-methyl-1H-tetrazol-5-yl)amino)pyrimidin-5-yl)-3,5-dihydroxyhept-6-enoate (13b). This compound was prepared from compound **5** and 1-methyl-1H-tetrazol-5-amine as described for compound **1b**. ¹H NMR (400 MHz, CD₃OD) δ 7.61 (2 H, dd, $J = 9.06, 5.54$ Hz),

7.15 (2 H, t, $J = 8.81$ Hz), 6.56 (1 H, dd, $J = 16.11, 1.51$ Hz), 5.51 (1 H, dd, $J = 16.11, 6.04$ Hz), 4.26–4.37 (1 H, m), 3.86–3.94 (1 H, m), 3.84 (3 H, s), 3.63 (3 H, s), 3.39–3.50 (1 H, m), 2.15–2.36 (2 H, m), 1.56–1.69 (1 H, m), 1.41–1.53 (1 H, m), 1.17 (6 H, d, $J = 7.05$ Hz); MS (ESI) m/z 486 (M + H)⁺; analytical HPLC (system A) $t_R = 2.84$ min, (system B) $t_R = 1.45$ min.

Sodium (3R,5S,E)-7-(4-(4-fluorophenyl)-6-isopropyl-2-(N-(1-methyl-1H-tetrazol-5-yl)methylsulfonamido)pyrimidin-5-yl)-3,5-dihydroxyhept-6-enoate (13c). This compound was prepared from compound **5** and 1-methyl-1H-tetrazol-5-amine as described for compound **1c**. ¹H NMR (400 MHz, CD₃OD) δ 7.77 (2 H, dd, $J = 9.1, 5.5$ Hz), 7.30 (2 H, t, $J = 8.8$ Hz), 6.73 (1 H, d, $J = 16.1$ Hz), 5.74 (1 H, dd, $J = 16.1, 6.0$ Hz), 4.48 (1 H, q, $J = 6.5$ Hz), 4.24 (3 H, s), 3.97–4.12 (1 H, m), 3.94 (3 H, s), 3.52–3.68 (1 H, m), 2.44 (1 H, dd, $J = 15.1, 5.0$ Hz), 2.36 (1 H, dd, $J = 15.6, 8.1$ Hz), 1.70–1.86 (1 H, m), 1.49–1.69 (1 H, m), 1.30 (3 H, d, $J = 6.5$ Hz), 1.29 (3 H, d, $J = 6.5$ Hz); MS (ESI) m/z 550 (M + H)⁺; analytical HPLC (system B) $t_R = 1.39$ min.

Sodium (3R,5S,E)-7-(2-(3-carboxy-1-methyl-1H-pyrazol-5-ylamino)-4-(4-fluorophenyl)-6-isopropylpyrimidin-5-yl)-3,5-dihydroxyhept-6-enoate (14a). This compound was prepared as described for compound **1** (via ethyl 5-amino-1-methyl-1H-pyrazole-3-carboxylate⁵¹). ¹H NMR (400 MHz, CD₃OD) δ 7.61 (2 H, dd, $J = 8.8, 5.3$ Hz), 7.13 (2 H, t, $J = 8.8$ Hz), 6.65 (1 H, s), 6.53 (1 H, d, $J = 16.1$ Hz), 5.45 (1 H, dd, $J = 16.1, 6.5$ Hz), 4.31 (1 H, q, $J = 6.0$ Hz), 3.85–4.00 (1 H, m), 3.77 (3 H, s), 3.37–3.46 (1 H, m), 2.31 (1 H, dd, $J = 15.1, 4.5$ Hz), 2.23 (1 H, dd, $J = 15.1, 7.1$ Hz), 1.58–1.68 (1 H, m), 1.42–1.51 (1 H, m), 1.22 (6 H, d, $J = 6.5$ Hz); MS (ESI) m/z 514 (M + H)⁺; analytical HPLC (system B) $t_R = 1.35$ min.

Acute Cholesterol Synthesis Assay in Rat. Inhibition of acute cholesterol synthesis in rats was determined essentially as previously described.⁵² Cholesterol synthesis, as measured by incorporation of ¹⁴C-acetate into hepatic sterols, was measured during a 4 h period spanning the peak of the mid-dark cycle in which HMG-CoA reductase levels are highest. Male Sprague–Dawley rats (Charles River) between 180 and 220 g were housed in a reverse light cycled room and were fed Purina rat chow (#5001) ad libitum for 7–10 days prior to use. Compounds, suspended in 0.5% carboxymethylcellulose (Sigma) in water, were dosed by oral gavage 2.5 h prior to the peak of the mid-dark cycle. Rats were injected intraperitoneally with (1-¹⁴C)-sodium acetate (1–3 mCi/mmol) 37.5 uCi/100 g body weight 30 min after receiving the oral dose. After 4 h, each group of 5 rats was sacrificed in a CO₂ chamber followed by immediate cervical dislocation and exsanguination by severing of the abdominal aorta. Excess blood was blotted, and a 1.0 g sample was removed from the left lobe of the liver and frozen at –20 °C in a borosilicate glass tube for subsequent analysis.

Lipids were extracted from livers by a modification of a previously described method.⁵³ Liver samples were mixed with 1.5 mL of 60% KOH in H₂O and 3 mL of methanol and heated at 85 °C in a water bath for 2 h, with mixing every half-hour. After cooling, 0.02 μ Ci (44 000 dpm) [$1\alpha, 2\alpha$ (n)-³H] cholesterol (1 μ Ci/ μ L, 39.0 Ci/mmol, Amersham Pharmacia Biotech) diluted with absolute ethanol from the stock was added to each sample as an internal control to monitor extraction efficiency. All samples, except 1 blank used for a control, were extracted with 7 mL of petroleum ether and centrifuged at 500g for 5 min at room temperature. The organic phase (4 mL) was collected into a scintillation vial. The aqueous phase was re-extracted with 3 mL of petroleum ether, and the organic phase (3 mL) was collected and pooled with the organic phase collected with the first extraction. Extracts were dried under nitrogen and resuspended in 0.5 mL of chloroform–methanol (2:1). Samples were then mixed with 10 mL of Opti-fluor scintillation fluid (Packard BioScience) and counted for both ³H and ¹⁴C using a Beckman LS3801 counter. This extraction procedure resulted in 50–90% recovery of the added ³H-cholesterol internal standard. Percent inhibition of cholesterol synthesis was then determined by comparing average ¹⁴C value from drug-treated animal groups with vehicle groups. Percent inhibition of cholesterol synthesis was plotted relative to the drug dose (mg/kg of animal), and an ED₅₀

value (level of drug required to suppress cholesterol synthesis *in vivo* by 50%) was calculated by best-fit analysis.

Weanling Rat Model of Myotoxicity. Female Sprague–Dawley rats (3 weeks, Charles River) were housed in a reverse light cycled room with 12 h dark/12 h light and fed Purina rat chow *ad libitum*. After 5 days of reverse light cycling, animals were weighed and dosed daily 2 h prior to mid-dark point of the light cycle with compounds suspended in 0.5% carboxymethylcellulose in water administered by oral gavage for 10 days. Animals were sacrificed by CO₂ asphyxiation 1 h after the last dose, blood was collected from the vena cava in 0.05% EDTA, and animals were perfused with 0.9% saline. Samples of skeletal muscle from the diaphragm, quadriceps, femoris, trapezius, and triceps brachii were collected in 10% neutral buffered formalin. Paraffin-embedded tissue sections (5 μm) were prepared, stained with hematoxylin and eosin, and subjected to histopathologic evaluation. Plasma levels of CK activity were measured using an autoanalyzer (Hitachi 912, Roche Diagnostics). A myotoxic signal was defined as dose-dependent CK elevations 2.5-fold above the mean value for the vehicle group or histopathologic evidence of myofiber necrosis in multiple segments of muscle tissue.

Acknowledgment. We greatly appreciate the support of Bristol-Myers Squibb Department of Discovery Analytical Sciences.

References

- (1) Third Report of the National Cholesterol Education Program (NCEP) Expert Panel on Detection, Evaluation, and Treatment of High Blood Cholesterol in Adults (Adult Treatment Panel III) final report. *Circulation* **2002**, *106*, 3143–3421.
- (2) Ross, S. D.; Allen, I. E.; Connelly, J. E.; Korenblat, B. M.; Smith, M. E.; Bishop, D.; Luo, D. Clinical outcomes in statin treatment: a meta-analysis. *Arch. Intern. Med.* **1999**, *159*, 1793–1802.
- (3) Brown, M. S.; Goldstein, J. L. A receptor-mediated pathway for cholesterol homeostasis. *Science* **1986**, *232* (4746), 34–47.
- (4) Horton, J. D.; Goldstein, J. L.; Brown, M. S. SREBPs: activators of the complete program of cholesterol and fatty acid synthesis in the liver. *J. Clin. Invest.* **2002**, *109*, 1125–1131.
- (5) Willard, A. K.; Smith, R. L.; Hoffman, W. F. 6(R)-[2-(8-Acyloxy-2-methyl-6-methyl (or hydrogen)-polyhydro-1-naphthyl)ethyl]-4(R)-hydroxy-3,4,5,6-tetrahydro-2H-pyran-2-ones, the hydroxy acid forms of these pyranones, salts and esters thereof, and a pharmaceutical antihypercholesterolemic composition containing them *Eur. Pat. Appl.*, EP 33538, 1981.
- (6) Tsujita, Y.; Kuroda, M.; Shimada, Y.; Tanzawa, K.; Arai, M.; Kaneko, I.; Tanaka, M.; Masuda, H.; Tarumi, C.; Watanabe, Y.; et al. CS-514, a competitive inhibitor of 3-hydroxy-3-methylglutaryl coenzyme A reductase: tissue-selective inhibition of sterol synthesis and hypolipidemic effect on various animal species. *Biochim. Biophys. Acta* **1986**, *877*, 50–60.
- (7) Endo, A.; Monacolin, K. A new hypocholesterolemic agent produced by a Monascus species. *J. Antibiot. (Tokyo)* **1979**, *32*, 852–854.
- (8) Kathawala, F. G. Analogs of mevalolactone and derivatives thereof and their use as pharmaceuticals. *PCT Int. Appl.*, WO 8402131, 1984.
- (9) Jones, P.; Kafonek, S.; Laurora, I.; Hunninghake, D. Comparative dose efficacy study of atorvastatin versus simvastatin, pravastatin, lovastatin, and fluvastatin in patients with hypercholesterolemia (the CURVES study). *Am. J. Cardiol.* **1998**, *81*, 582–587.
- (10) Roth, B. D. Preparation of trans-6-[(carbamoypyrrolyl)alkyl]-4-hydroxypyranones as hypocholesterolemic. US Patent 4,681,893, 1987.
- (11) Angerbauer, R.; Fey, P.; Huebsch, W.; Philipps, T.; Bischoff, H.; Petzinna, D.; Schmidt, D. Preparation of 7-[4-(4-fluorophenyl)-2,6-diisopropyl-5-methoxymethylpyrid-3-yl]-3,5-dihydroxy-6-heptenoate isomers as HMG-CoA reductase inhibitors. Ger. Offen, DE 4040026, 1992.
- (12) Hirai, K.; Ishiba, T.; Koike, H.; Watanabe, M. Pyrimidine derivatives as HMG-CoA reductase inhibitors. *Eur. Pat. Appl.*, EP 521471, 1993.
- (13) Blasetto, J. W.; Stein, E. A.; Brown, W. V.; Chitra, R.; Raza, A. Efficacy of rosuvastatin compared with other statins at selected starting doses in hypercholesterolemic patients and in special population groups. *Am. J. Cardiol.* **2003**, *91* (5A), 3C–10C; discussion 10C.
- (14) Brousseau, M. E. Statins, super-statins and cholesterol absorption inhibitors. *IDrugs* **2003**, *6*, 458–463.
- (15) Stein, E. A.; Strutt, K.; Southworth, H.; Diggle, P. J.; Miller, E. Comparison of rosuvastatin versus atorvastatin in patients with heterozygous familial hypercholesterolemia. *Am. J. Cardiol.* **2003**, *92*, 1287–1293.
- (16) Thompson, P. D.; Clarkon, P.; Karas, R. H. Statin-associated myopathy. *JAMA* **2003**, *289*, 1681–1690.
- (17) Ballantyne, C. M.; Corsini, A.; Davidson, M. H.; Holdaas, H.; Jacobson, T. A.; Leitersdorf, E.; Marz, W.; Reckless, J. P.; Stein, E. A. Risk for myopathy with statin therapy in high-risk patients. *Arch. Intern. Med.* **2003**, *163*, 553–564.
- (18) Hamilton-Craig, I. Statin-associated myopathy. *Med. J. Aust.* **2001**, *175*, 486–489.
- (19) Omar, M. A.; Wilson, J. P.; Cox, T. S. Rhabdomyolysis and HMG-CoA reductase inhibitors. *Ann Pharmacother* **2001**, *35*, 1096–1107.
- (20) Arora, R.; Liebo, M.; Maldonado, F. Statin-induced myopathy: the two faces of Janus. *J. Cardiovasc. Pharmacol. Ther.* **2006**, *11*, 105–112.
- (21) Chapman, M. J.; Carrie, A. Mechanisms of statin-induced myopathy: a role for the ubiquitin-proteasome pathway. *Arterioscler. Thromb. Vasc. Biol.* **2005**, *25*, 2441–2444.
- (22) Flint, O. P.; Masters, B. A.; Gregg, R. E.; Durham, S. K. HMG CoA reductase inhibitor-induced myotoxicity: pravastatin and lovastatin inhibit the geranylgeranylation of low-molecular-weight proteins in neonatal rat muscle cell culture. *Toxicol. Appl. Pharmacol.* **1997**, *145*, 99–110.
- (23) Nezasa, K.; Higaki, K.; Takeuchi, M.; Nakano, M.; Koike, M. Uptake of rosuvastatin by isolated rat hepatocytes: comparison with pravastatin. *Xenobiotica* **2003**, *33*, 379–388.
- (24) Schachter, M. Chemical, pharmacokinetic and pharmacodynamic properties of statins: an update. *Fundam. Clin. Pharmacol.* **2005**, *19*, 117–125.
- (25) Recently, researchers from Pfizer have also reported on their efforts to find efficacious and less myotoxic statins. (a) Pfefferkorn, J. A.; Choi, C.; Larsen, S. D.; Auerbach, B.; Hutchings, R.; Park, W.; Askev, V.; Dillon, L.; Hanselman, J. C.; Lin, Z.; Lu, G. H.; Robertson, A.; Sekerke, C.; Harris, M. S.; Pavlovsky, A.; Bainbridge, G.; Caspers, N.; Kowala, M.; Tait, B. D. Substituted pyrazoles as hepatoselective HMG-CoA reductase inhibitors: discovery of (3R,5R)-7-[2-(4-fluorophenyl)-4-isopropyl-5-(4-methyl-benzylcarbamoyl)-2H-pyrazol-3-yl]-3,5-dihydroxyheptanoic acid (PF-3052334) as a candidate for the treatment of hypercholesterolemia. *J. Med. Chem.* **2008**, *51*, 31–45. (b) Pfefferkorn, J. A.; Song, Y.; Sun, K.-L.; Miller, S. R.; Trivedi, B. K.; Choi, C.; Sorenson, R. J.; Bratton, L. D.; Unangst, P. U.; Larsen, S. D.; et al. Design and synthesis of hepatoselective, pyrrole-based HMG-CoA reductase inhibitors. *Bioorg. Med. Chem. Lett.* **2007**, *17*, 4538–4544.
- (26) Istvan, E. S.; Deisenhofer, J. Structural mechanism for statin inhibition of HMG-CoA reductase. *Science* **2001**, *292* (5519), 1160–1164.
- (27) Compound **1b** was built without the dihydroxy acid tail from the rosuvastatin ligand crystal structure as a starting point and was quantum-mechanically minimized with DFT-B3LYP(6-31G*) using Jaguar (Maestro v. 80110, Schrodinger LLC, 2007). The resulting structure was attached to the dihydroxy acid tail from rosuvastatin, and the compound was docked rigidly into the rosuvastatin HMGR structure using Glide (Maestro v. 80110, Schrodinger LLC, 2007) with vdW radii of nonpolar receptor atoms scaled by 0.9, all other parameters default, to produce the structure shown in Figure 2.
- (28) Watanabe, M.; Koike, H.; Ishiba, T.; Okada, T.; Seo, S.; Hirai, K. Synthesis and biological activity of methanesulfonamide pyrimidine- and N-methanesulfonyl pyrrole-substituted 3,5-dihydroxy-6-heptenoates, a novel series of HMG-CoA reductase inhibitors. *Bioorg. Med. Chem.* **1997**, *5*, 437–444.
- (29) Blakemore, P. R.; Cole, W. J.; Kocienski, P. J.; Morley, A. A stereoselective synthesis of trans-1,2-disubstituted alkenes based on the condensation of aldehydes with metalated 1-phenyl-1H-tetrazol-5-yl sulfones. *Synlett* **1998**, *1*, 26–28.
- (30) Julia, M.; Paris, J. M. Syntheses with the help of sulfones V. General method of synthesis of double bonds. *Tetrahedron Lett.* **1973**, *49*, 4833–4836.
- (31) Brodfuehrer, P. R.; Sattelberg, T. R.; Kant, J.; Qian, X. Process for preparing chiral diol sulfones and dihydroxy acid HMG CoA reductase inhibitors. *PCT Int. Appl.*, WO 2002098854.
- (32) Madsen, C. S.; Janovitz, E.; Cuff, C. C.; Zhang, R.; Nguyen-Tran, N.; Ryan, C. S.; Yin, X.; Monshizadegan, H.; Chang, M.; D'Arienzo, C.; Scheer, S.; Setters, R.; Search, D.; Chen, X.; Zhuang, S.; Harrity, T.; Apedo, A.; Huang, C.; Kowala, M.; Blonar, M. A.; Sun, C.-Q.; Robl, J. A.; Stein, P. D. The guinea pig as a preclinical model for demonstrating the efficacy and safety of statins. *J. Pharmacol. Exp. Ther.* **2008**, *324*, 576–586.
- (33) Zhao, Y.; Jona, J.; Chow, D. T.; Rong, H.; Semin, D.; Xia, X.; Zanon, R.; Spancake, C.; Maliski, E. High-throughput/low-p measurement using parallel liquid chromatography/ultraviolet/mass spectrometry and sample-pooling. *Rapid Commun. Mass. Spectrom.* **2002**, *16*, 1548–1555.

- (34) Davidson, M. H. Rosuvastatin: a highly efficacious statin for the treatment of dyslipidaemia. *Expert Opin. Investig. Drugs* **2002**, *11*, 125–141.
- (35) Edwards, P. A.; Lemongello, D.; Fogelman, A. M. Improved methods for the solubilization and assay of hepatic 3-hydroxy-3-methylglutaryl coenzyme A reductase. *J. Lipid Res.* **1979**, *20*, 40–46.
- (36) Capuzzi, D. M.; Margolis, S. Metabolic studies in isolated rat liver cells. I. Lipid synthesis. *Lipids* **1971**, *6*, 601–608.
- (37) Conde, K.; Pineda, G.; Newton, R. S.; Fernandez, M. L. Hypocholesterolemic effects of 3-hydroxy-3-methylglutaryl coenzyme A (HMG-CoA) reductase inhibitors in the guinea pig: atorvastatin versus simvastatin. *Biochem. Pharmacol.* **1999**, *58*, 1209–1219.
- (38) Suzuki, H.; Aoki, T.; Tamaki, T.; Sato, F.; Kitahara, M.; Saito, Y. Hypolipidemic effect of NK-104, a potent HMG-CoA reductase inhibitor, in guinea pigs. *Atherosclerosis* **1999**, *146*, 259–270.
- (39) Guinea pig, similar to human up-regulates LDL receptor in response to statin treatment: Conde, K.; Vergara-Jimenez, M.; Krause, B. R.; Newton, R. S.; Fernandez, M. L. Hypocholesterolemic actions of atorvastatin are associated with alterations on hepatic cholesterol metabolism and lipoprotein composition in the guinea pig. *J. Lipid Res.* **1996**, *37*, 2372–2382.
- (40) Measurement of CK levels from a second dose–response study of **1b** ($n = 8$ animals/group) in guinea pigs revealed one incident ($>2.5\times$) within the lowest dose group (10 mg/kg) with a value of 1104 U/L. This value also represented the highest plasma CK value for any of the **1b**-treated animals. With the exception of this isolated incident, no other instances ($>2.5\times$) were observed at any dose up to 100 mg/kg. The mean CK levels for the 0, 10, 25, 50, 75, and 100 mg/kg doses were 366.6, 456.8, 420.8, 350.8, 429.0, and 432.3, respectively. None of the values were determined to be statistically significant ($p < 0.05$). The clear lack of a dose-dependent increase in CK strongly suggests that the isolated incident identified within the 10 mg/kg dose group was an anomaly and most likely not the result of drug treatment. Unusually high CK levels were also observed for one animal in the control group for the atorvastatin study. It is possible that elevated CK level in this particular animal resulted from trauma, possibly due to fighting or excessive struggling during dosing. Histopathologic analyses of muscle tissues obtained from the **1b**-treated animals revealed that there were no myopathic lesions for any group.
- (41) Armitage, J. The safety of statins in clinical practice. *Lancet* **2007**, *370*, 1781–1790.
- (42) Kornbrust, D. J.; MacDonald, J. S.; Peter, C. P.; Duchai, D. M.; Stubbs, R. J.; Germershausen, J. I.; Alberts, A. W. Toxicity of the HMG-coenzyme A reductase inhibitor, lovastatin, to rabbits. *J. Pharmacol. Exp. Ther.* **1989**, *248*, 498–505.
- (43) Reijneveld, J. C.; Koot, R. W.; Bredman, J. J.; Joles, J. A.; Bar, P. R. Differential effects of 3-hydroxy-3-methylglutaryl-coenzyme A reductase inhibitors on the development of myopathy in young rats. *Pediatr. Res.* **1996**, *39*, 1028–1035.
- (44) Smith, P. F.; Eydeloth, R. S.; Grossman, S. J.; Stubbs, R. J.; Schwartz, M. S.; Germershausen, J. I.; Vyas, K. P.; Kari, P. H.; MacDonald, J. S. HMG-CoA reductase inhibitor-induced myopathy in the rat: cyclosporine A interaction and mechanism studies. *J. Pharmacol. Exp. Ther.* **1991**, *257*, 1225–1235.
- (45) Rebuffat, P.; Belloni, A. S.; Cavallini, L.; Mazzocchi, G.; Meneghelli, V.; Nussdorfer, G. G. Effect of mevinolin on rat hepatocytes: a morphometric study. *Exp. Pathol.* **1988**, *35* (3), 133–139.
- (46) The correlation of in vitro cell selectivity and hydrophilicity described above has certain limitations. The fact that the slightly more lipophilic simvastatin ($\log P = 4.8$) has a better safety profile in the clinic than cerivastatin ($\log P = 4.5$) suggests that factors beyond lipophilicity are likely to play critical roles for statin-induced myotoxicity. Such factors may include relative potencies, differences in metabolism, and differences in peripheral exposure (Evans, M. Rees, A. Effects of HMG-CoA reductase inhibitors on skeletal muscle: Are all statins the same? *Drug Safety* **2002**, *25*, 649–663.). Simvastatin is dosed as a lactone prodrug and is reported to have higher levels of liver extraction in rat (Nezasa, K.-I. Higaki, K. Matsumura, T. Inazawa, K. Hasegawa, H. Nakano, M. Koike, M. Liver-specific distribution of rosuvastatin in rats: Comparison with pravastatin and simvastatin. *Drug Metab. Dispos.* **2002**, *30*, 1158–1163.) and human (Igel, M. Sudhop, T. Bergmann, K. V. Metabolism and drug interactions of 3-hydroxy-3-methylglutaryl coenzyme A-reductase inhibitors (statins). *Eur. J. Clin. Pharmacol.* **2001**, *57*, 357–364.) compared to other marketed statins, thus minimizing peripheral exposure. In addition to hepatic clearance, drug metabolism may also play an important role in statin-induced myopathy. Atorvastatin is dosed as a relatively lipophilic parent drug that is metabolized by cytochrome P450 3A4 into equally active more polar hydroxy metabolites (Lea, A. P. Mctavish, D. Atorvastatin a review of its pharmacology and therapeutic potential in the management of hyperlipidemias. *Drugs* **1997**, *53*, 828–847). It has been hypothesized that the more polar, active metabolites, which are less likely to penetrate the myocyte cell membrane, are responsible for the relatively low incidence of myopathy observed in the clinic (Wierzbicki, A. S. Atorvastatin. *Exp. Opin. Pharmacother.* **2001**, *2*, 819–830).
- (47) Igel, M.; Sudhop, T.; von Bergmann, K. Pharmacology of 3-hydroxy-3-methylglutaryl-coenzyme A reductase inhibitors (statins), including rosuvastatin and pitavastatin. *J. Clin. Pharmacol.* **2002**, *42*, 835–845.
- (48) Li, T.; Reeves, R. Placebo-controlled, ascending single-dose study to evaluate the safety, pharmacokinetics, and pharmacodynamics of BMS-644950 in healthy subjects. Internal Report MB106001; Department of Clinical Discovery, Bristol-Myers Squibb, Research & Development.
- (49) Martin, P. D.; Mitchell, P. D.; Schneck, D. W. Pharmacodynamic effects and pharmacokinetics of a new HMG-CoA reductase inhibitor, rosuvastatin, after morning or evening administration in healthy volunteers. *Br. J. Clin. Pharmacol.* **2002**, *54*, 472–477.
- (50) Kroger, C.; Schoknecht, G.; Beyer, H. 1,2,4-Triazoles. VI. *Chem. Ber.* **1964**, *97* (2), 396–404.
- (51) Vanotti, F.; Villa, M. Synthesis of novel derivatives of 1H-imidazol[1,2-b]pyrazole as potential CNS-agents. *J. Heterocycl. Chem.* **1994**, *31*, 737–743.
- (52) Alberts, A. W.; Chen, J.; Kuron, G.; Hunt, V.; Huff, J.; Hoffman, C.; Rothrock, J.; Lopez, M.; Joshua, H.; Harris, E.; Patchett, A.; Monaghan, R.; Currie, S.; Stapley, E.; Albers-Schonberg, G.; Hensens, O.; Hirshfield, J.; Hoogsteen, K.; Liesch, J.; Springer, J. Mevinolin: a highly potent competitive inhibitor of hydroxymethylglutaryl-coenzyme A reductase and a cholesterol-lowering agent. *Proc. Natl. Acad. Sci. U.S.A.* **1980**, *77*, 3957–3961.
- (53) Dugan, R. E.; Slakey, L. L.; Briedis, A. V.; Porter, J. W. Factors affecting the diurnal variation in the level of 3-hydroxy-3-methylglutaryl coenzyme A reductase and cholesterol-synthesizing activity in rat liver. *Arch. Biochem. Biophys.* **1972**, *152*, 21–27.

JM800001N